Investigating potential therapeutic targets, biomarkers, and preclinical models in malignant solid tumors

Doctoral thesis

to obtain a doctorate (PhD)

from the Faculty of Medicine

of the University of Bonn

Racha Hosni

from Damascus, Syria

2026

Written with authorization of

the Faculty of Medicine of the University of Bonn

First reviewer: Prof. Dr. med Marieta Toma

Second reviewer: Prof. Dr. Eva Kiermaier

Day of oral examination: 23.03.2026

From the Institute of Pathology, University Hospital Bonn

Table of Contents

List of abbreviations

ADC	Antibody-Drug Conjugate
BRAF	B-Raf Proto-Oncogene, Serine/Threonine Kinase
BTC	Biliary Tract Cancer
CCA	Cholangiocarcinoma
CD	Cluster of Differentiation
CTLA-4	Cytotoxic T-Lymphocyte Associated Protein 4
dCCA	Distal Cholangiocarcinoma
dMMR	Mismatch Repair Deficient
eCCA	Extrahepatic Cholangiocarcinoma
FGFR2	Fibroblast Growth Factor Receptor 2
FOLFOX	5-Fluorouracil-Leucovorine-Oxaliplatin
GBC	Gall Bladder Carcinoma
HCC	Hepatocellular Carcinoma
HER2	Human Epidermal Growth Factor Receptor 2
HER3	Human Epidermal Growth Factor Receptor 3
iCCA	Intrahepatic Cholangiocarcinoma
IDH1	Isocitrate Dehydrogenase 1
KIT	KIT Proto-Oncogene, Receptor Tyrosine Kinase
LAT1	Lymphocyte Activating 3
MEK1/2	Mitogen-Activated Protein Kinase Kinase 1/2
MSI-H	Microsatellite Instability-High
mTNBC	Metastatic Triple-Negative Breast Cancer
NECTIN4	Nectin Cell Adhesion Molecule 4
NRAS	NRAS Proto-Oncogene, Gtpase
PARP	Poly ADP-Ribose Polymerase
PARPi	Poly ADP-Ribose Polymerase Inhibitor
PDOs	Patient-Derived Organoids
pCCA	Perihilar Cholangiocarcinoma
PD-1	Programmed Cell Death 1

PDAC	Pancreatic Ductal Adenocarcinoma
PEG	Polyethylene Glycol
PFS	Progression-Free Survival
PSC	Primary Sclerosing Cholangitis
SLC7A5	Solute Carrier Family 7 Member 5
TACE	Transarterial Chemoembolization
TCGA	The Cancer Genome Atlas
T-DM1	Ado-Trastuzumab Emtansine
TROP2	Trophoblast Cell-Surface Antigen 2
UV	Ultraviolet

1. Abstract

As malignant diseases remain to be associated with high morbidity and mortality, the search for more effective therapeutics and biomarkers is a critical medical need. Research efforts in the last decade have led to the development of a novel and more physiological *in vitro* cancer model called patient-derived organoids (PDOs), which are cultured 3-dimentional self-organizing multi-cell structures generated from cancer stem cells. This thesis aimed to investigate potential novel therapeutic targets, employing in-house established PDOs, and predictive biomarkers in solid malignant tumors. In the first publication, we revealed that the TROP2 protein is frequently expressed in cholangiocarcinoma and that cholangiocarcinoma PDOs are highly susceptible to sacituzumab govitecan, an antibody-drug conjugate targeting TROP2. Using TROP2-knockout cholangiocarcinoma cell lines, we also demonstrated the target-dependent and target-independent mechanisms of action. Given that sacituzumab govitecan is a clinically-approved medication, used for the treatment of breast cancer, with a known safety profile in humans, our data suggests that sacituzumab govitecan could be repurposed for the treatment of cholangiocarcinoma patients. In my second publication, we established a novel protocol for generating PDOs from melanoma brain metastases and demonstrated that their response to targeted therapy (BRAF and MEK inhibitors) *in vitro* matched the mutational profile of the original tumor samples, implying that they represent an accurate model for predicting patient responses as well as for efficient targeted drug screening. In my third publication, we demonstrated that the expression of the amino acid transporter *SLC7A5*/LAT1 in tumor cells and in intra-tumoral immune cells is associated with shorter overall survival in a cohort of biliary tract cancer. Moreover, we revealed that its expression in intra-tumoral immune cells is higher in primary-sclerosing cholangitis associated- biliary tract cancer (PSC-BTC) compared to sporadic biliary tract cancer. These results suggest that *SLC7A5*/LAT1 could represent a prognostic biomarker in BTC, and demonstrates differences in the immune cells' phenotype between sporadic and PSC-associated BTC. Taken together, the findings of these studies could potentially improve the therapy, management, and/or prognosis of cholangiocarcinoma patients. Moreover, the proposed PDO culture model of melanoma brain metastases could pave the way for novel drug development for this advanced disease.

2. Introduction and aims with references

2.1 Biliary tract cancer (BTC)

Biliary tract cancer (BTC) is a highly heterogenous cancer originating from cholangiocytes, which form the specialized epithelia that lines the bile ducts. BTC arises in the gall bladder or cystic duct (gall bladder carcinoma (GBC)) or in the biliary tree (cholangiocarcinoma (CCA)) (Banales et al., 2019; Komuta, 2024; Vogel et al., 2023). CCA is conventionally classified based on the anatomical location into intrahepatic (iCCA), perihilar (pCCA); also known as Klatskin tumor, and distal (dCCA) (Razumilava and Gores, 2012). Briefly, iCCA occurs in the intrahepatic bile ducts excluding the right and left hepatic ducts, pCCA arises from the right and left hepatic ducts and the common hepatic duct, while dCCA occurs in the common bile duct (choledochus) marked by the insertion of the cystic duct (Brindley et al., 2021; Kendall et al., 2019; Komuta, 2024). Extrahepatic CCA (eCCA) comprises both pCCA and dCCA. iCCA has been reclassified by the 5th WHO classification (2019) of tumors of the digestive system based on the histology of the affected bile ducts into large and small duct subtypes (Nagtegaal et al., 2019).

2.2 BTC incidence and prognosis

Although BTC is considered to be one of the rare cancer types, accounting for 1% of all human cancers, incidence and mortality have been on the rise worldwide in the last decade, especially for the intrahepatic subtypes. Notably, the age-standardized incidence of CCA varies greatly across the globe due to differences in endemic and local risk factors. For example, the age-standardized incidence is about 85 per 100,000 in Thailand and about 3 per 100,000 in Germany (Banales et al., 2020; Khan et al., 2019). CCA is the second most common primary liver cancer after hepatocellular carcinoma (HCC), comprising around 15% of all primary liver cancers (Banales et al., 2020; Vogel et al., 2023). Patient prognosis remains dismal which is mainly due to 1. high tumor recurrence rates after surgical resection, and 2. disease is diagnosed at already advanced, tumor unresectable stages, in more than 70% of the patients (Banales et al., 2020). The current 5-year survival rate for CCA patients ranges between 2-23% depending on the tumor

stage; however, this estimate is expected to increase given the new advances in therapeutic approaches (Banales et al., 2020; Kang et al., 2022; Wang et al., 2024).

2.3 BTC Risk factors

About half of CCA cases in the Western world are attributed to one or more risk factors, while the remaining cases are completely sporadic without any identifiable etiologies (Khan et al., 2019). Some known risk factors are shared for all subtypes of CCAs, while others are more specific to a subtype or a geographical location. Notably, chronic inflammation of the liver and/or biliary system is a characteristic that is shared by most of those risk factors (Banales et al., 2020; Brindley et al., 2021; Khan et al., 2019). In Western countries, primary sclerosing cholangitis (PSC), a chronic inflammation of the intrahepatic and extrahepatic bile ducts, is the most well-known risk factor for all anatomic subtypes of CCA. (Brindley et al., 2021; Khan et al., 2019; Vogel et al., 2023). The risk of gall bladder cancer generally increases with age; and cholelithiasis and cholecystitis represent the main predisposing factors (Vogel et al., 2023).

2.4 Therapeutic strategies and current guidelines for BTC

2.4.1 management of early-stage BTC

Surgery is currently the only curative approach, aiming to achieve resection with no tumor at the margin (R0). However, this aim is in some cases impossible leading to high rates of R1 resections. Additionally, the recurrence rate after curative-intent resection remains very high (around 80% in the first 3 years after surgery). Accordingly, adjuvant chemotherapy with capecitabine with or without adjuvant radiotherapy is recommended for BTC patients following surgical tumor resection (Vogel et al., 2023).

2.4.2 management of locally-advanced BTC

For locally-advanced unresectable tumors without metastasis, treatment options include locoregional or systemic therapy (Alvaro et al., 2023; Vogel et al., 2023). Currently, the first-line systemic therapy for BTC is a combination of gemcitabine and cisplatin with immune checkpoint inhibitors like durvalumab or pembrolizumab, which target PD-L1 and PD-1, respectively (Zanuso et al., 2024). Locoregional therapy includes tumor ablation, a procedure in which chemical or energy-based cytotoxic sources are locally applied to a tumor, as well as intra-arterial therapies, such as hepatic arterial chemotherapy infusion,

transarterial chemoembolization (TACE), and selective internal radiotherapy (Ahmed et al., 2014; Edeline et al., 2021; Pang et al., 2024; Vogel et al., 2023). Patients who respond well to locoregional or systemic therapy should be re-considered for eligibility for surgical resection.

2.4.3 management of advanced and metastatic BTC

The current standard of care for first-line treatment of advanced or metastatic BTC is a combinatorial chemo-immunotherapy regimen consisting of gemcitabine and cisplatin plus durvalumab or pembrolizumab, and is associated with a median overall survival of 12.9 and 12.7 months; respectively (Kelley et al., 2023; Oh et al., 2024; Zanuso et al., 2024). The second-line treatment options include chemotherapy (5-fluorouracil-leucovorine-oxaliplatin (FOLFOX)); immunotherapy (permbrolizumab for mismatch repair deficient (dMMR) or microsatellite instability-high (MSI-H) tumors); and targeted therapy for patients with tumors harboring specific genetic alterations, as detailed in the following section (Vogel et al., 2023).

2.4.4 targeted therapy

It is estimated that nearly 40% of BTCs harbor genetic alterations that are potentially druggable. It is therefore recommended to perform mutational profiling for advanced BTC tumors as early as possible to assess eligibility for targeted therapies as second-line treatment options (Lamarca et al., 2020; Vogel et al., 2023; Zanuso et al., 2024). Currently, available targeted therapy is directed towards tumors harboring isocitrate dehydrogenase 1 (*IDH1*) mutations, fibroblast growth factor receptor 2 (*FGFR2*) fusions, human epidermal growth factor receptor 2 (*HER2*) overexpression, and proto-oncogene B-Raf (*BRAF*) mutations (Vogel et al., 2023; Zanuso et al., 2024).

2.5 Antibody-drug conjugates (ADCs)

Antibody-drug conjugates (ADCs) are a promising class of cancer therapeutics generally aiming at selective antibody-mediated delivery of chemotherapeutic drugs to tumor cells, thereby enhancing efficacy and simultaneously reducing toxicity. An ADC is made up of three main components; namely, a monoclonal antibody, a chemotherapeutic drug payload, and a linker which conjugates the antibody to the drug payload. ADCs do not represent a novel treatment modality per se; the first ADC clinical trial for the treatment of

cancer in humans dates back to the 1980s; however, recent improvements in the molecular design of ADCs, especially in the choice of linkers and the conjugation chemistry, have led to remarkable enhancements in drug activity and responses (Tarantino et al., 2022). Initial ADC approvals were in the context of hematological malignancies. Gemtuzumab ozogamicin was the very first ADC to receive FDA approval in 2000 for the treatment of CD33-positive acute myeloid leukemia (Baron and Wang, 2018; Tarantino et al., 2022). Later, in 2013, ado-trastuzumab emtansine (T-DM1) was the first ADC to receive FDA approval for the treatment of solid tumors (HER2-positive metastatic breast cancer) (Amiri-Kordestani et al., 2014; Tarantino et al., 2022). Currently, there are a total of 13 ADCs approved for the treatment of solid tumors (Jian et al., 2025).

2.6 Biomarkers

A biomarker is defined as a biological molecule found in body fluids or tissue that indicates the presence of a normal physiological condition or a disease state (Henry and Hayes, 2012; Passaro et al., 2024). In the field of oncology, cancer biomarkers identify characteristics of the disease and currently represent indispensable tools for the screening, diagnosis, prognosis, as well as in the prediction of how a specific cancer is likely to respond to a given treatment (prognostic/predictive biomarkers). Accordingly, biomarkers facilitate the personalized medicine approaches by guiding physicians in the choice of the therapeutic option based on the cancer’s unique molecular profile (Passaro et al., 2024).

2.7 Melanoma

Melanoma is a malignant tumor arising from melanocytes, which are intraepithelial cells originating from neural crests and specialized in melanin production. Melanoma occurring in the skin, also known as cutaneous melanoma, represents the most common type of melanoma (>90%). Less common types include mucosal and uveal melanomas which occur on mucosal membranes and in the uvea of the eyes; respectively (Long et al., 2023).

2.8 Melanoma incidence and risk factors

The incidence of cutaneous melanoma has been rising steadily in fair skin populations, such as in the USA, Europe, and Australia, which may be due to the increased ultraviolet (UV) radiation exposure as well as to the increased skin screening programs resulting in

enhanced disease detection. On the contrary, melanoma-associated deaths have decreased since 2013 which is likely due to the implementation of more effective therapy regimens for advanced melanoma (Berk-Krauss et al., 2020; Long et al., 2023). In addition to genetic predisposition, UV exposure has been identified as a major risk factor as well as a major carcinogen in melanomagenesis. UV radiation has been shown to induce DNA mutations in proto-oncogenes; namely, *BRAF*, *NRAS*, and *KIT*, which are identified as driver mutations in over 75% of cutaneous melanoma cases (Amaral et al., 2025; Conforti and Zalaudek, 2021; Ghissassi et al., 2009; Long et al., 2023).

2.9 Melanoma treatment and prognosis

Patients with localized cutaneous melanoma generally have a very good prognosis and are treated with wide local excision of the primary tumor (Amaral et al., 2025; Waseh and Lee, 2023). Advanced melanoma (stages 3 and 4), that is not eligible for surgical resection, is currently treated using immune checkpoint blockade targeting PD-1 (nivolumab, pembrolizumab) alone or in combination with CTLA-4 blockade (ipilimumab), or in combination with LAG-3 blockade (relatlimab) (Amaral et al., 2025). Melanomas with the *BRAF*-V600 mutation are treated with BRAF inhibitors (dabrafenib) combined with MEK inhibitors (trametinib) (Amaral et al., 2025). Despite the advances in the therapeutic strategies for the treatment of metastatic melanoma, patients still have a poor prognosis (around 30% 5-year survival rate) (Waseh and Lee, 2023). Importantly, stage 4 melanoma is one of the most common cancer types causing brain metastases which are particularly challenging to manage (Tawbi et al., 2018).

2.10 Patient-derived organoid models (PDOs)

The discovery and implementation of novel drugs for the treatment of human cancer diseases continues to be a critical need. However, the success rate of transitioning preclinical drug candidates into clinical use, often referred to as “bench-to-bedside translation”, has been very low (around 10%) which is likely attributed to drawbacks in the standard models commonly used in preclinical cancer research, namely 2D cell lines and mice models (Hay et al., 2014; Kamb, 2005; Porter et al., 2020). Cancers’ heterogeneity and complexity represent the main challenges in efficiently modelling these diseases *in vitro* and *in vivo* (Kamb, 2005; Porter et al., 2020). Consequently, several innovative

models addressing these challenges are being developed. One such model is patient-derived tumor organoids (also known as PDOs), which are 3D cell cultures generated from a patient's tumor resection specimen or biopsy. Organoids are self-assembling and self-organizing 3D multi-cell structures derived from adult tissue-resident stem cells, including cancer stem cells, as well as embryonic and induced pluripotent stem cells. Organoids are regarded as near-physiological models since they are shown to recapitulate the genetic, cellular, pathophysiological characteristics, as well as the heterogeneity of the tumor tissue they are derived from (Driehuis et al., 2020; Porter et al., 2020). As such, PDOs currently represent attractive models for preclinical cancer research, including drug screening studies. A multitude of published studies describe the use of PDOs as efficient *in vitro* models for cancer drug screening, and many provide evidence on their high potential to accurately predict patient responses, making them valuable tools for both drug screening and personalized medicine approaches (Driehuis et al., 2020; Tuveson and Clevers, 2019). For instance, a cutting-edge study published in 2018 on pancreatic ductal adenocarcinoma (PDAC) has shown a high molecular concordance between the original tumor and the matched PDOs (Tiriac et al., 2018). Moreover, the study reports a retrospective analysis which shows that the *in vitro* chemotherapy sensitivity profiles of the generated PDAC PDOs recapitulates clinical patient responses (Tiriac et al., 2018).

2.11 Aims

The aim of this thesis was to investigate potential novel therapeutic targets and predictive biomarkers in solid malignant tumors, employing state-of-the-art *in vitro* cancer models. In the first publication, the expression of the protein targets of the recently-developed ADCs was evaluated in cholangiocarcinoma. Subsequently, based on the initial finding that TROP2 is frequently expressed at high levels in cholangiocarcinoma, the efficacy and mechanisms-of-action of sacituzumab govitecan, an ADC targeting TROP2, were tested *in vitro* using cholangiocarcinoma patient-derived tumor organoids as well as cancer cell lines. In the second publication, patient-derived organoids were established from melanoma-brain metastases, and their feasibility for predicting targeted-therapy responses, based on the mutational status of the original tumors, was evaluated. In the third publication, the expression of SLC7A5/LAT1, an amino acid transporter, was

evaluated on the protein and transcriptomic levels as a potential prognostic biomarker in cholangiocarcinoma.

2.12 References

Ahmed, M., Solbiati, L., Brace, C.L., Breen, D.J., Callstrom, M.R., Charboneau, J.W., Chen, M.-H., Choi, B.I., Baère, T. de, Gerald D Dodd, I.I.I., Dupuy, D.E., Gervais, D.A., Gianfelice, D., Gillams, A.R., Fred T Lee, J., Leen, E., Lencioni, R., Littrup, P.J., Livraghi, T., Lu, D.S., McGahan, J.P., Meloni, M.F., Nikolic, B., Pereira, P.L., Liang, P., Rhim, H., Rose, S.C., Salem, R., Sofocleous, C.T., Solomon, S.B., Soulen, M.C., Tanaka, M., Vogl, T.J., Wood, B.J., Goldberg, S.N., For the International Working Group on Image-guided Tumor Ablation, I.O.S.F.E.P., 2014. Image-guided Tumor Ablation: Standardization of Terminology and Reporting Criteria—A 10-Year Update. Radiology 273, 241. https://doi.org/10.1148/radiol.14132958

Alvaro, D., Gores, G.J., Walicki, J., Hassan, C., Sapisochin, G., Komuta, M., Forner, A., Valle, J.W., Laghi, A., Ilyas, S.I., Park, J.-W., Kelley, R.K., Reig, M., Sangro, B., 2023. EASL-ILCA Clinical Practice Guidelines on the management of intrahepatic cholangiocarcinoma. Journal of Hepatology 79, 181–208. https://doi.org/10.1016/j.jhep.2023.03.010

Amaral, T., Ottaviano, M., Arance, A., Blank, C., Chiarion-Sileni, V., Donia, M., Dummer, R., Garbe, C., Gershenwald, J.E., Gogas, H., Guckenberger, M., Haanen, J., Hamid, O., Hauschild, A., Höller, C., Lebbé, C., Lee, R.J., Long, G.V., Lorigan, P., Couselo, E.M., Nathan, P., Robert, C., Romano, E., Schadendorf, D., Sondak, V., Suijkerbuijk, K.P.M., Akkooi, A.C.J. van, Michielin, O., Ascierto, P.A., 2025. Cutaneous melanoma: ESMO Clinical Practice Guideline for diagnosis, treatment and follow-up☆. Annals of Oncology 36, 10–30. https://doi.org/10.1016/j.annonc.2024.11.006

Amiri-Kordestani, L., Blumenthal, G.M., Xu, Q.C., Zhang, L., Tang, S.W., Ha, L., Weinberg, W.C., Chi, B., Candau-Chacon, R., Hughes, P., Russell, A.M., Miksinski, S.P., Chen, X.H., McGuinn, W.D., Palmby, T., Schrieber, S.J., Liu, Q., Wang, J., Song, P., Mehrotra, N., Skarupa, L., Clouse, K., Al-Hakim, A., Sridhara, R., Ibrahim, A., Justice, R., Pazdur, R., Cortazar, P., 2014. FDA approval: ado-trastuzumab emtansine for the treatment of patients with HER2-positive metastatic breast cancer. Clin Cancer Res 20, 4436–4441. https://doi.org/10.1158/1078-0432.CCR-14-0012

Banales, J.M., Huebert, R.C., Karlsen, T., Strazzabosco, M., LaRusso, N.F., Gores, G.J., 2019. Cholangiocyte pathobiology. Nat Rev Gastroenterol Hepatol 16, 269–281. https://doi.org/10.1038/s41575-019-0125-y

Banales, J.M., Marin, J.J.G., Lamarca, A., Rodrigues, P.M., Khan, S.A., Roberts, L.R., Cardinale, V., Carpino, G., Andersen, J.B., Braconi, C., Calvisi, D.F., Perugorria, M.J., Fabris, L., Boulter, L., Macias, R.I.R., Gaudio, E., Alvaro, D., Gradilone, S.A., Strazzabosco, M., Marzioni, M., Coulouarn, C., Fouassier, L., Raggi, C., Invernizzi, P., Mertens, J.C., Moncsek, A., Rizvi, S., Heimbach, J., Koerkamp, B.G., Bruix, J., Forner, A., Bridgewater, J., Valle, J.W., Gores, G.J., 2020.

Cholangiocarcinoma 2020: the next horizon in mechanisms and management. Nature Reviews Gastroenterology & Hepatology 17, 557–588. https://doi.org/10.1038/s41575-020-0310-z

Baron, J., Wang, E.S., 2018. Gemtuzumab ozogamicin for the treatment of acute myeloid leukemia. Expert Rev Clin Pharmacol 11, 549–559. https://doi.org/10.1080/17512433.2018.1478725

Berk-Krauss, J., Stein, J.A., Weber, J., Polsky, D., Geller, A.C., 2020. New Systematic Therapies and Trends in Cutaneous Melanoma Deaths Among US Whites, 1986-2016. Am J Public Health 110, 731–733. https://doi.org/10.2105/AJPH.2020.305567

Brindley, P.J., Bachini, M., Ilyas, S.I., Khan, S.A., Loukas, A., Sirica, A.E., Teh, B.T., Wongkham, S., Gores, G.J., 2021. Cholangiocarcinoma. Nat Rev Dis Primers 7, 1–17. https://doi.org/10.1038/s41572-021-00300-2

Conforti, C., Zalaudek, I., 2021. Epidemiology and Risk Factors of Melanoma: A Review. Dermatol Pract Concept 11, e2021161S. https://doi.org/10.5826/dpc.11S1a161S

Driehuis, E., Kretzschmar, K., Clevers, H., 2020. Establishment of patient-derived cancer organoids for drug-screening applications. Nat Protoc 15, 3380–3409. https://doi.org/10.1038/s41596-020-0379-4

Edeline, J., Lamarca, A., McNamara, M.G., Jacobs, T., Hubner, R.A., Palmer, D., Koerkamp, B.G., Johnson, P., Guiu, B., Valle, J.W., 2021. Locoregional therapies in patients with intrahepatic cholangiocarcinoma: A systematic review and pooled analysis. Cancer Treatment Reviews 99. https://doi.org/10.1016/j.ctrv.2021.102258

Ghissassi, F.E., Baan, R., Straif, K., Grosse, Y., Secretan, B., Bouvard, V., Benbrahim-Tallaa, L., Guha, N., Freeman, C., Galichet, L., Cogliano, V., 2009. A review of human carcinogens—Part D: radiation. The Lancet Oncology 10, 751–752. https://doi.org/10.1016/S1470-2045(09)70213-X

Hay, M., Thomas, D.W., Craighead, J.L., Economides, C., Rosenthal, J., 2014. Clinical development success rates for investigational drugs. Nat Biotechnol 32, 40–51. https://doi.org/10.1038/nbt.2786

Henry, N.L., Hayes, D.F., 2012. Cancer biomarkers. Molecular Oncology 6, 140–146. https://doi.org/10.1016/j.molonc.2012.01.010

Jian, A., Zhao, G., Zhou, J., Wang, S., Li, N., 2025. How to Design Next-generation of Antibody-Drug Conjugates for Cancer Treatment: Lessons from Unsuccessful Clinical Trials. Cancer Letters 217535. https://doi.org/10.1016/j.canlet.2025.217535

Kamb, A., 2005. What's wrong with our cancer models? Nat Rev Drug Discov 4, 161–165. https://doi.org/10.1038/nrd1635

Kang, M.J., Lim, J., Han, S.-S., Park, H.M., Kim, S.-W., Lee, W.J., Woo, S.M., Kim, T.H., Won, Y.-J., Park, S.-J., 2022. Distinct prognosis of biliary tract cancer according to tumor location, stage, and treatment: a population-based study. Sci Rep 12, 10206. https://doi.org/10.1038/s41598-022-13605-3

Kelley, R.K., Ueno, M., Yoo, C., Finn, R.S., Furuse, J., Ren, Z., Yau, T., Klümpen, H.-J., Chan, Stephen L., Ozaka, M., Verslype, C., Bouattour, M., Park, J.O., Barajas, O., Pelzer, U., Valle, J.W., Yu, L., Malhotra, U., Siegel, A.B., Edeline, J., Vogel, A., Akce, M., Diaz, I.A., Alves, G., Anand, S., Arslan, C., Asselah, J., Assenat, E., Aubin, F., Bai, L.-Y., Bai, Y., Barajas, O., Bates, S., Begbie, S., Ben-Aharon, I., Beri, N., Berres, M.-L., Blanc, J.-F., Borbath, I., Bordonaro, R., Bouattour, M.,

Brandi, G., Burgoyne, A., Butthongkomvong, K., Camandaroba, M., Cao, K., Carballido, M., Chan, Stephan Lam, Chen, J.-S., Chen, M.-H., Chen, X., Cheng, A., Chiu, T.-J., Choi, H.J., Chon, H.J., Collignon, J., Gracian, A.C., Davis, S., Carvalho, R.S. de, Groot, D.J.A. de, Demols, A., Vos, J.D., Diab, M., Easaw, J., Eatock, M., Edeline, J., Elias, R., Eskens, F., Falcone, A., Fernandez, P., Finn, R., Franke, F., Furukawa, M., Furuse, J., Gbolahan, O., Geboes, K., Geneser, K.-L., Geng, Z., Geva, R., Gillmore, R., Goetze, T., Gou, H., Grasselli, J., Gu, S., Gumus, M., Mohammad, N.H., Hao, C., Harputluoglu, H., Hatoum, H., Heinemann, V., Ho, W.K., Hsu, C., Hubert, A., Hwang, J., Inanc, M., Iseas, S., Jeyasingam, V., Fonseca, P.J., Joubert, W., Juengsamarn, J., Kaen, D., Kanai, M., Kasper-Virchow, S., Kazemi, G., Kelleher, F., Kelley, R., Kim, J.W., Kim, J.G., Abrahao, A.B.K., Klumpen, H., Kochenderfer, M., Kose, F., Lam, H.C., Lee, C., Lee, H.W., Lee, M., Lee, M.A., Lee, W.M.S., Sourd, S.L., Li, D., Li, W., Liang, H., Liang, T., Lim, C.S., Lingerfelt, B., Lopez, C., Low, J., Mercade, T.M., Malka, D., Mao, Y., Masi, G., McCune, S., McDermott, R., McWhirter, E., Mendez, G., Milella, M., Mizuno, N., Mizutani, T., Moniz, C., Morales, L., Martin, A.J.M., Nervi, B., Ngamphaiboon, N., Oh, S.C., Oksuzoglu, B., Outlaw, D., Ozaka, M., Ozguroglu, M., Ozyilkan, O., Painemal, C., Pan, Y., Park, J.O., Pelzer, U., Peng, C., Petorin, C., Pezet, D., Power, D., Qin, S., Ren, Z., Roohullah, A., Ryu, H., Salman, P., Sasaki, M., Sasidharan, R., Satoh, T., Schulze, K., Scott-Brown, M., Segovia, R., Seufferlein, T., Siena, S., Sinapi, I., Smolenschi, C., Song, T., Sookprasert, A., Soparattanapaisarn, N., Starling, N., Stein, S., Stemmer, S., Su, H., Sugimoto, R., Suksomboon charoen, T., Tam, V., Tan, A.L., Tan, C.K., Tanasanvimon, S., Tonini, G., Tortora, G., Tsuji, A., Ueno, M., Uribe, R., Venerito, M., Mata, H.V., Verslype, C., Victorino, A.P., Vogel, A., Wade, J., Waldschmidt, D.T., Wang, L., Isahk, W.Z.W., Wasan, H., Weschenfelder, R., Wong, C.Y., Wong, Y.F., Yalcin, S., Weber, P.Y., Yang, X., Yasui, H., Yau, T., Yazici, O., Yen, C.-J., Ying, J., Yoo, C., Yu, W., Zhao, H., 2023. Pembrolizumab in combination with gemcitabine and cisplatin compared with gemcitabine and cisplatin alone for patients with advanced biliary tract cancer (KEYNOTE-966): a randomised, double-blind, placebo-controlled, phase 3 trial. The Lancet 401, 1853–1865. https://doi.org/10.1016/S0140-6736(23)00727-4

Kendall, T., Verheij, J., Gaudio, E., Evert, M., Guido, M., Goeppert, B., Carpino, G., 2019. Anatomical, histomorphological and molecular classification of cholangiocarcinoma. Liver International 39, 7–18. https://doi.org/10.1111/liv.14093

Khan, S.A., Tavolari, S., Brandi, G., 2019. Cholangiocarcinoma: Epidemiology and risk factors. Liver International 39, 19–31. https://doi.org/10.1111/liv.14095

Komuta, M., 2024. Intrahepatic cholangiocarcinoma: histological diversity and the role of the pathologist. JLC 24, 17–22. https://doi.org/10.17998/jlc.2023.12.11

Lamarca, A., Barriuso, J., McNamara, M.G., Valle, J.W., 2020. Molecular targeted therapies: Ready for “prime time” in biliary tract cancer. Journal of Hepatology 73, 170–185. https://doi.org/10.1016/j.jhep.2020.03.007

Long, G.V., Swetter, S.M., Menzies, A.M., Gershenwald, J.E., Scolyer, R.A., 2023. Cutaneous melanoma. The Lancet 402, 485–502. https://doi.org/10.1016/S0140-6736(23)00821-8

Nagtegaal, I.D., Odze, R.D., Klimstra, D., Paradis, V., Rugge, M., Schirmacher, P., Washington, K.M., Carneiro, F., Cree, I.A., Board, the W.C. of T.E., 2019. The

2019 WHO classification of tumours of the digestive system. Histopathology 76, 182. https://doi.org/10.1111/his.13975

Oh, D.-Y., He, A.R., Bouattour, M., Okusaka, T., Qin, S., Chen, L.-T., Kitano, M., Lee, C.-K., Kim, J.W., Chen, M.-H., Suksomboon charoen, T., Ikeda, M., Lee, M.A., Chen, J.-S., Potemski, P., Burris, H.A., Ostwal, V., Tanasanvimon, S., Morizane, C., Zaucha, R.E., McNamara, M.G., Avallone, A., Cundom, J.E., Breder, V., Tan, B., Shimizu, S., Tougeron, D., Evesque, L., Petrova, M., Zhen, D.B., Gillmore, R., Gupta, V.G., Dayyani, F., Park, J.O., Buchschacher, G.L., Rey, F., Kim, H., Wang, J., Morgan, C., Rokutanda, N., Żotkiewicz, M., Vogel, A., Valle, J.W., 2024. Durvalumab or placebo plus gemcitabine and cisplatin in participants with advanced biliary tract cancer (TOPAZ-1): updated overall survival from a randomised phase 3 study. Lancet Gastroenterol Hepatol 9, 694–704. https://doi.org/10.1016/S2468-1253(24)00095-5

Pang, C., Li, J., Dou, J., Li, Z., Li, L., Li, K., Chen, Q., An, C., Zhou, Z., He, G., Lou, K., Liang, F., Xi, H., Wang, X., Zuo, M., Cheng, Z., Han, Z., Liu, F., Yu, X., Yu, J., Jiang, X., Yang, M., Liang, P., 2024. Microwave ablation versus liver resection for primary intrahepatic cholangiocarcinoma within Milan criteria: a long-term multicenter cohort study. eClinicalMedicine 67. https://doi.org/10.1016/j.eclinm.2023.102336

Passaro, A., Al Bakir, M., Hamilton, E.G., Diehn, M., André, F., Roy-Chowdhuri, S., Mountzios, G., Wistuba, I.I., Swanton, C., Peters, S., 2024. Cancer biomarkers: Emerging trends and clinical implications for personalized treatment. Cell 187, 1617–1635. https://doi.org/10.1016/j.cell.2024.02.041

Porter, R.J., Murray, G.I., McLean, M.H., 2020. Current concepts in tumour-derived organoids. Br J Cancer 123, 1209–1218. https://doi.org/10.1038/s41416-020-0993-5

Razumilava, N., Gores, G.J., 2012. Classification, Diagnosis, and Management of Cholangiocarcinoma. Clinical gastroenterology and hepatology : the official clinical practice journal of the American Gastroenterological Association 11, 13. https://doi.org/10.1016/j.cgh.2012.09.009

Tarantino, P., Carmagnani Pestana, R., Corti, C., Modi, S., Bardia, A., Tolaney, S.M., Cortes, J., Soria, J.-C., Curigliano, G., 2022. Antibody-drug conjugates: Smart chemotherapy delivery across tumor histologies. CA Cancer J Clin 72, 165–182. https://doi.org/10.3322/caac.21705

Tawbi, H.A., Boutros, C., Kok, D., Robert, C., McArthur, G., 2018. New Era in the Management of Melanoma Brain Metastases. Am Soc Clin Oncol Educ Book 741–750. https://doi.org/10.1200/EDBK_200819

Tiriac, H., Belleau, P., Engle, D.D., Plenker, D., Deschênes, A., Somerville, T.D.D., Froeling, F.E.M., Burkhart, R.A., Denroche, R.E., Jang, G.-H., Miyabayashi, K., Young, C.M., Patel, H., Ma, M., LaComb, J.F., Palmaira, R.L.D., Javed, A.A., Huynh, J.C., Johnson, M., Arora, K., Robine, N., Shah, M., Sanghvi, R., Goetz, A.B., Lowder, C.Y., Martello, L., Driehuis, E., LeComte, N., Askan, G., Iacobuzio-Donahue, C.A., Clevers, H., Wood, L.D., Hruban, R.H., Thompson, E., Aguirre, A.J., Wolpin, B.M., Sasson, A., Kim, J., Wu, M., Bucobo, J.C., Allen, P., Sejpal, D.V., Nealon, W., Sullivan, J.D., Winter, J.M., Gimotty, P.A., Grem, J.L., DiMaio, D.J., Buscaglia, J.M., Grandgenett, P.M., Brody, J.R., Hollingsworth, M.A., O'Kane, G.M., Notta, F., Kim, E., Crawford, J.M., Devoe, C., Ocean, A., Wolfgang, C.L., Yu, K.H., Li, E., Vakoc, C.R., Hubert, B., Fischer, S.E., Wilson, J.M., Moffitt,

R., Knox, J., Krasnitz, A., Gallinger, S., Tuveson, D.A., 2018. Organoid Profiling Identifies Common Responders to Chemotherapy in Pancreatic Cancer. Cancer Discov 8, 1112–1129. https://doi.org/10.1158/2159-8290.CD-18-0349

Tuveson, D., Clevers, H., 2019. Cancer modeling meets human organoid technology. Science 364, 952–955. https://doi.org/10.1126/science.aaw6985

Vogel, A., Bridgewater, J., Edeline, J., Kelley, R.K., Klümpen, H.J., Malka, D., Primrose, J.N., Rimassa, L., Stenzinger, A., Valle, J.W., Ducreux, M., 2023. Biliary tract cancer: ESMO Clinical Practice Guideline for diagnosis, treatment and follow-up☆. Annals of Oncology 34, 127–140. https://doi.org/10.1016/j.annonc.2022.10.506

Wang, Y., Alsaraf, Y., Bandaru, S.S., Lyons, S., Reap, L., Ngo, T., Yu, Z., Yu, Q., 2024. Epidemiology, survival and new treatment modalities for intrahepatic cholangiocarcinoma. Journal of Gastrointestinal Oncology 15. https://doi.org/10.21037/jgo-24-165

Waseh, S., Lee, J.B., 2023. Advances in melanoma: epidemiology, diagnosis, and prognosis. Front. Med. 10. https://doi.org/10.3389/fmed.2023.1268479

Zanuso, V., Tesini, G., Valenzi, E., Rimassa, L., 2024. New systemic treatment options for advanced cholangiocarcinoma. JLC 24, 155–170. https://doi.org/10.17998/jlc.2024.08.07

3 Publications

3.1 Publication 1: The Antibody–Drug Conjugate Sacituzumab Govitecan (IMMU-132) Represents a Potential Novel Therapeutic Strategy in Cholangiocarcinoma / https://doi.org/10.1158/1535-7163.MCT-24-0972

Note: this publication is not included in the dissertation for legal reasons.

3.2 Publication 2: Melanoma Brain Metastases Patient-Derived Organoids: An In Vitro Platform for Drug Screening / https://doi.org/10.3390/pharmaceutics16081042

pharmaceutics

MDPI

Article

Melanoma Brain Metastases Patient-Derived Organoids: An In Vitro Platform for Drug Screening

Saif-Eldin Abedellatif [1,*], Racha Hosni [1], Andreas Waha [2], Gerrit H. Gielen [2], Mohammed Banat [3], Motaz Hamed [3], Erdem Güresir [3], Anne Fröhlich [4], Judith Sirokay [4], Anna-Lena Wulf [1], Glen Kristiansen [1], Torsten Pietsch [2], Hartmut Vatter [3], Michael Hölzel [5], Matthias Schneider [3] and Marieta Ioana Toma [1,*]

[1] Institute of Pathology, University Hospital Bonn, 53127 Bonn, Germany; racha.hosni@ukbonn.de (R.H.); annalena.wulf@ukbonn.de (A.-L.W.); glen.kristiansen@ukbonn.de (G.K.)
[2] Institute for Neuropathology, University Hospital Bonn, 53127 Bonn, Germany; andreas.waha@ukbonn.de (A.W.); gerrit.gielen@ukbonn.de (G.H.G.); torsten.pietsch@ukbonn.de (T.P.)
[3] Department of Neurosurgery, University Hospital Bonn, 53127 Bonn, Germany; mohammed.banat@ukbonn.de (M.B.); motaz.hamed@ukbonn.de (M.H.); erdem.gueresir@medizin.uni-leipzig.de (E.G.); hartmut.vatter@ukbonn.de (H.V.); matthias.schneider@ukbonn.de (M.S.)
[4] Department of Dermatology, University Hospital Bonn, 53127 Bonn, Germany; anne.froehlich@ukbonn.de (A.F.); judith.sirokay@ukbonn.de (J.S.)
[5] Institute of Experimental Oncology, University Hospital Bonn, 53127 Bonn, Germany; michael.hoelzel@ukbonn.de
* Correspondence: s4saabed@uni-bonn.de (S.-E.A.); marieta.toma@ukbonn.de (M.I.T.); Tel.: +49-22828715371 (M.I.T.)

Abstract: Background and aims: Brain metastases are prevalent in the late stages of malignant melanoma. Multimodal therapy remains challenging. Patient-derived organoids (PDOs) represent a valuable pre-clinical model, faithfully recapitulating key aspects of the original tumor, including the heterogeneity and the mutational status. This study aimed to establish PDOs from melanoma brain metastases (MBM-PDOs) and to test the feasibility of using them as a model for in vitro targeted-therapy drug testing. Methods: Surgical resection samples from eight patients with melanoma brain metastases were used to establish MBM-PDOs. The samples were enzymatically dissociated followed by seeding into low-attachment plates to generate floating organoids. The MBM-PDOs were characterized genetically, histologically, and immunohistologically and compared with the parental tissue. The MBM-PDO cultures were exposed to dabrafenib (*BRAF* inhibitor) and trametinib (*MEK* inhibitor) followed by a cell viability assessment. Results: Seven out of eight cases were successfully cultivated, maintaining the histological, immunohistological phenotype, and the mutational status of the parental tumors. Five out of seven cases harbored *BRAF* V600E mutations and were responsive to *BRAF* and *MEK* inhibitors in vitro. Two out of seven cases were *BRAF* wild type: one case harboring an *NRAS* mutation and the other harboring a *KIT* mutation, and both were resistant to *BRAF* and *MEK* inhibitor therapy. Conclusions: We successfully established PDOs from melanoma brain metastases surgical specimens, which exhibited a consistent histological and mutational profile with the parental tissue. Using FDA-approved *BRAF* and *MEK* inhibitors, our data demonstrate the feasibility of employing MBM-PDOs for targeted-therapy in vitro testing.

Keywords: melanoma; brain metastases; *BRAF*; organoids

Citation: Abedellatif, S.-E.; Hosni, R.; Waha, A.; Gielen, G.H.; Banat, M.; Hamed, M.; Güresir, E.; Fröhlich, A.; Sirokay, J.; Wulf, A.-L.; et al. Melanoma Brain Metastases Patient-Derived Organoids: An In Vitro Platform for Drug Screening. *Pharmaceutics* **2024**, *16*, 1042. https://doi.org/10.3390/pharmaceutics16081042

Academic Editor: Gabriele Grassi

Received: 4 July 2024
Revised: 28 July 2024
Accepted: 31 July 2024
Published: 5 August 2024

1. Importance of This Study

The incidence of malignant melanoma is rising worldwide. Although the five-year survival rate for early-stage melanoma is over 90%, in advanced metastatic stages it decreases to 10%. About 60% of patients with melanoma develop brain metastases; however, those patients are excluded from clinical trials, which hinders the development of new therapeutic approaches for this group of patients. Additionally, the biology of melanoma

brain metastases is poorly understood due to the lack of representative research models; hence, there is a critical need to develop novel faithful models. In this study, melanoma brain metastases' patient-derived organoid culture lines were established from surgical specimens. The organoid cultures faithfully recapitulated the histological and mutational profile of the parental tissue. Drug-sensitivity experiments using the FDA-approved *BRAF* and *MEK* inhibitors, dabrafenib and trametinib, demonstrated the feasibility of employing melanoma brain metastases patient-derived organoids as models for targeted-therapy in vitro testing and for the discovery of novel therapeutic targets.

2. Introduction

Brain metastases are one of the most common and challenging neurologic complications of cancer. It is estimated that approximately 20% of individuals diagnosed with cancer develop brain metastases [1]. Among these metastatic brain lesions, melanoma stands as the third most frequent cause, accounting for 6–11% of all cases after lung cancer (41%) and breast cancer (19%) [2,3]. Up to 60% of patients with melanoma develop brain metastasis during disease progression. The management of advanced-stage cancer, especially after the development of brain metastases, necessitates a comprehensive and multimodal treatment approach, including surgery, radiotherapy, chemotherapy, immunotherapy, and targeted therapy based on the mutational status [1]. *BRAF* is the gene most commonly affected by point mutations in cutaneous melanoma, which in turn leads to the constitutive activation of the MAPK pathway [4]. This promotes tumor progression, but, on the other hand, it represents a molecular target for therapy using *MAPK* inhibitors, such as *BRAF* and *MEK* inhibitors, which have shown response rates of up to 76% in patients with melanomas harboring *BRAF* mutations [5,6]. The development and the integration of immune checkpoint inhibitors, specifically PD-1 inhibitors (nivolumab and pembrolizumab) and the CTLA-4 blocking antibody (ipilimumab) as combination therapy have significantly improved clinical outcomes for advanced and metastatic melanoma [7,8].

Although checkpoint inhibitors result in long-time survival in some patients with metastatic malignant melanoma, regardless of the *BRAF* mutational status [9], only a group of patients show this favorable response to therapy and these cannot be identified beforehand so far. To understand and decipher the complex nature of melanoma-derived brain metastases, it is essential to establish robust and representative models of melanoma brain metastases that can be generated efficiently. Patient-derived organoid (PDO) models recapitulate the original tumor in terms of tissue architecture and maintain the genetic and histological characteristics of the primary tumor and the intratumoral heterogeneity [10,11]. Therefore, PDO models have emerged as a promising in vitro platform serving diverse research purposes, such as biomarker discovery, personalized medicine, and drug screening, providing enhanced insights into tumor biology and the evaluation of responses to novel therapeutic agents [12]. In this study, we successfully established PDO cultures derived from seven surgical samples of melanoma brain metastases (MBMs), which faithfully retained the genetic and histological characteristics of the primary tumor. Furthermore, the established MBM-PDO cultures were treated in vitro with targeted therapies, *BRAF* and *MEK* inhibitors, to ascertain whether they can accurately predict targeted-therapy responses based on their mutational profile.

3. Material and Methods

3.1. Human Specimens

Informed consent was obtained from patients undergoing craniotomies for brain metastases between 2022 and 2023 in the Department of Neurosurgery, University Hospital Bonn. The experiments were approved by the Ethics Committee of the Medical Faculty, University Bonn (#417/17 with amendment from 2020; #169/23). The clinical–pathological characteristics are given in Table 1. The median age at the surgery for brain metastases was 55 years. The primary diagnostic was conducted at the Institute for Neuropathology, Uni-

versity Hospital Bonn. Two patients had brain metastases as the first tumor manifestation, while the other six patients experienced brain metastases at an advanced stage (Table 1).

Table 1. Clinico-pathological characteristics of the patients included in this study.

Characteristics			Number (%)
Sex		Male	5 (62.5%)
		Female	3 (37.5%)
Localization		Frontal	4 (50%)
		Parietal	3 (37.5%)
		Occipital	1 (12.5%)
Number of brain metastases		Singular	6 (75%)
		Multiple	2 (25%)
Extracranial metastases		0	5 (62.5%)
		Pulmonary	1 (12.5%)
		Osseous	2 (25%)
TNM *	T	pTx (first diagnosis)	2 (25%)
		pT1	0 (0%)
		pT2	1 (12.5%)
		pT3	4 (50%)
		pT4	1 (12.5%)
	N	pN0	5 (62.5%)
		pN1	2 (25%)
		pN2	1 (12.5%)
	M	pM1	8 (100%)
Mutation		BRAF V600E	5 (62.5%)
		BRAF wild type	3 (37.5%)
Therapy	Pre-neurosurgical resection	Stereotactic radiotherapy	3 (37.5%)
		Interferon therapy	2 (25%)
		Combination immunotherapy	3 (37.5%)
	Post-neurosurgical resection	BRAF and MEK inhibitor (tafinlar, mekinist)	2 (25%)
		Combination immunotherapy (nivolumab, ipilimumab)	3 (37.5%)

* TNM classification: T (tumor) represents the size and extent of the primary tumor; N (node) represents the involvement of regional lymph nodes; M (metastasis) represents the presence of distant metastasis.

3.2. Human Tumor Collection

Tumor tissues were collected in basis medium ((Advanced DMEM/F12 supplemented with 1× GlutaMax)), 10 mM HEPES solution (Carl Roth, Karlsruhe, Germany), 100 µg/mL Normocin (InvivoGen, San Diego, CA, USA), and 2.5 µg/mL Amphotericin B (Biowest, Nuaillé, France). The tumor samples were manually cut with scissors followed by further mechanical dissociation using gentleMACS™ C Tubes and the gentleMACS™ Octo Dissociator (Miltenyi Biotec, Bergisch Gladbach, Germany). After filtering the tumor samples using a 1000 µm filter, red blood cell lysis was performed using RBC Lysing Buffer Hybri-Max (Sigma-Aldrich, St. Louis, MO, USA). The resultant cell suspensions were then cryopreserved at −80 °C using CryoStor CS10 media (Stemcell Technologies, Vancouver, BC, Canada) until the completion of pathological evaluation and tumor mutational analysis of the primary brain metastasis at the Institute for Neuropathology, University Hospital Bonn.

3.3. MBM-PDO Floating Culture

The cryopreserved dissociated tumor samples were thawed and digested in an enzyme mix (1 mg/mL collagenase IV (Rockland Immunochemicals, Limerick, PA, USA)), 15 µg/mL DNase (ThermoFisherScientific, Waltham, MA, USA), and 10 µM Y-27632-HCL Rock inhibitor (Biogems, Westlake Village, CA, USA) in basis medium, at 37 °C for 1 h followed by incubation with 3–5 mL TrypLE Express (Gibco, ThermoFisherScientific, Waltham, MA, USA), and filtered through a 70 µm cell strainer (Avantor, Radnor Township, PA, USA). The cells were seeded in ultra-low attachment (ULA) plates (Stemcell Technologies, Vancouver, BC, Canada) in melanoma brain metastases patient-derived organoid (MBM-PDO) culture media (Supplementary Table S1) and cultured in a humidified cell culture incubator (37 °C, 5% CO_2). The MBM-PDO culture media was refreshed every three days. MBM-PDO cultures were observed daily, photographed every four days, and passaged every 3–4 weeks.

3.4. Splitting of PDO Cultures

The MBM-PDO cultures were gently transferred from the ULA plates using a pipette, washed several times in basis medium, centrifuged, and resuspended in 3–5 mL of TrypLE Express (Gibco, ThermoFisher Scientific, Waltham, MA, USA) and incubated at 37 °C for 10 min. After washing the organoids with basis medium supplemented with 10% FCS, the cell pellet was resuspended in MBM-PDO culture medium, seeded in ultra-low attachment (ULA) plates (Stemcell Technologies, Vancouver, BC, Canada), and incubated at 37 °C.

3.5. Embedding of PDO Cultures

The MBM-PDO cultures were fixed in 4% paraformaldehyde (PFA) overnight at 4 °C, pelleted, and embedded using HistoGel (Richard-Allan Scientific, San Diego, CA, USA). The samples were allowed to cool and solidify at 4 °C for one day and were then embedded in paraffin following standard protocols.

3.6. Immunohistochemistry

For immunohistochemistry (IHC) staining, 2 µm thick sections were cut, deparaffinized, and pre-treated according to the standard protocols in the immunohistochemistry laboratory of the Institute of Pathology. Immunohistochemistry was performed on the Medac platform (Melan A: Agilent, clone A103, dilution 1:100; S100:Medac/Cell Marque, clone 4C4.9, dilution 1:2000; HMB45: Agilent, clone HMB45, dilution 1:400; Ki67: Zytomed, mouse anti-human, dilution 1:250, clone K-2; CD8: Agilent; clone C8/144B, dilution 1:50) or on the Ventana platform (CD4: Roche, clone SP35, ready-to-use-antibody). Slides were counterstained with hematoxylin and examined under the microscope (Olympus BX 50) for the evaluation of reactivity.

3.7. Mutational Analysis

The mutational analysis for brain metastases was conducted either by next-generation sequencing (NGS) (Institute of Pathology) or pyrosequencing (Institute of Neuropathology). For primary tumors, DNA from the paraffin-embedded material was extracted using the Maxwell RSC DNA FFPE Kit (Promega, Madison, WI, USA). DNA isolation from the organoids was carried out using the DNeasy Blood and Tissue kit (Qiagen, Hilden, Germany).

3.8. Next-Generation Sequencing (NGS)

DNA was eluted in 120 µL nuclease-free water, and the concentration was determined on a Quantus™ fluorometer using the QuantiFluor® ONE ds DNA System (Promega). Generation of the sequencing library was performed using a QIAseq™ targeted DNA custom panel (Qiagen) with an input of 40 ng DNA. The amplification products were subjected to next-generation sequencing on an Illumina MiSeq sequencer (Illumina, San

Diego, CA, USA). The sequencing data were analyzed for genomic variants using the CLC Genomics Workbench/Server 23 (Qiagen Bioinformatics).

3.9. Pyrosequencing of BRAF Codon 600

Pyrosequencing was used to determine the sequence at hotspot codon 600 of the *BRAF* gene. A 122 bp fragment of *BRAF*-exon 15 was amplified using following primers *BRAF*-forward 5′-GAAGACCTCACAGTAAAAATAG-3′ and *BRAF*-reverse 5′-Biotin-ATAGCCTC AATTCTTACCATCC-3′. PCR was performed with the Pyromark PCR Kit (Qiagen) with 15 min at 95 °C, followed by 40 cycles of 94 °C, 60 °C, and 72 °C for 30 s each, and finally, 72 °C for 10 min. Single-stranded DNA templates were purified on Streptavidin Sepharose High-Performance beads (GE Healthcare, Chicago, IL, USA) using the PSQ Vacuum Prep Tool and Worktable (Biotage, Uppsala, Sweden). Pyrosequencing was performed using PyroMark® Gold Reagents (Qiagen) on the Pyromark Q24 instrument (Biotage) with the pyrosequencing primer 5′-AGGTGATTTTGGTCTAGCTA-3′. Positive and negative controls were used to compare the results. The pyrograms were analyzed by PyroMark Q24 software Method 003 (Version number 1.0.10, serial number 000019, Biotage) using the allele quantification (AQ) module to determine the percentage of mutant versus wild-type alleles according to percentage relative peak height.

3.10. Treatment with BRAF and MEK Inhibitors

To evaluate drug sensitivity, MBM-PDO cultures were seeded into a low attachment 96-well cell culture plate (SARSTEDT AG & CO. KG, Nümbrecht, Germany) with 50 µL of MBM-PDO culture medium in each well. After 24 h of culture, 50 µL of the treatment medium was added to the organoid cultures. These cultures were subjected to a combination therapy of BRAF and MEK inhibitors (dabrafenib (Cayman Chemical, Ann Arbor, MI, USA) and trametinib (MCE MedChemExpress, Monmouth Junction, NJ, USA)), at various concentrations (1 µM, 0.5 µM, 0.25 µM, and 0.125 µM).

3.11. Measurement of Intracellular ATP

After 72 h of drug treatment, the intracellular level of ATP was measured by a Cell Titer-Glo 3D assay (Promega, G9682). Briefly, 100 µL of the Cell Titer-Glo reagent was added to each well followed by incubation at room temperature on an orbital shaker for one hour to ensure adequate cell lysis. After incubation, 100 µL samples were transferred to a white Nunc MicroWell 96-Well, Nunclon Delta-Treated, Flat-Bottom Microplate (Thermo Scientific, Waltham, MA, USA). Luminescence measurements were conducted using a SPARK microplate reader (TECAN, Männedorf, Switzerland) with an integration time of 500 ms at the Institute of Experimental Oncology, University Hospital Bonn. The relative viability was calculated as a percentage, normalized to the vehicle control.

4. Results

4.1. Establishment and Cultivation of MBM-PDOs

To establish PDOs from melanoma brain metastases, we developed a 3D culture protocol that did not rely on tissue extracellular matrices such as Matrigel or collagen (Figure 1A). The PDO cultures were successfully established from MBM samples in seven out of eight cases (Figure 1B), resulting in an overall success rate of 87.5%. We could cultivate metastases from previously untreated as well as from previously treated brain melanoma metastases (Table 1).

The PDO cultures from different patients exhibited a range of distinct morphologies, which were discernible by light microscopy examination of the histological hematoxylin and eosin (H&E)-stained sections (Figure 1C). Some of these cultures displayed a spherical structure with elongated well-defined borders, while others exhibited a rounded structure, or less structured organoids positioned adjacent to each other (Figure 1C). The intra-culture morphological variance of the PDOs was very low.

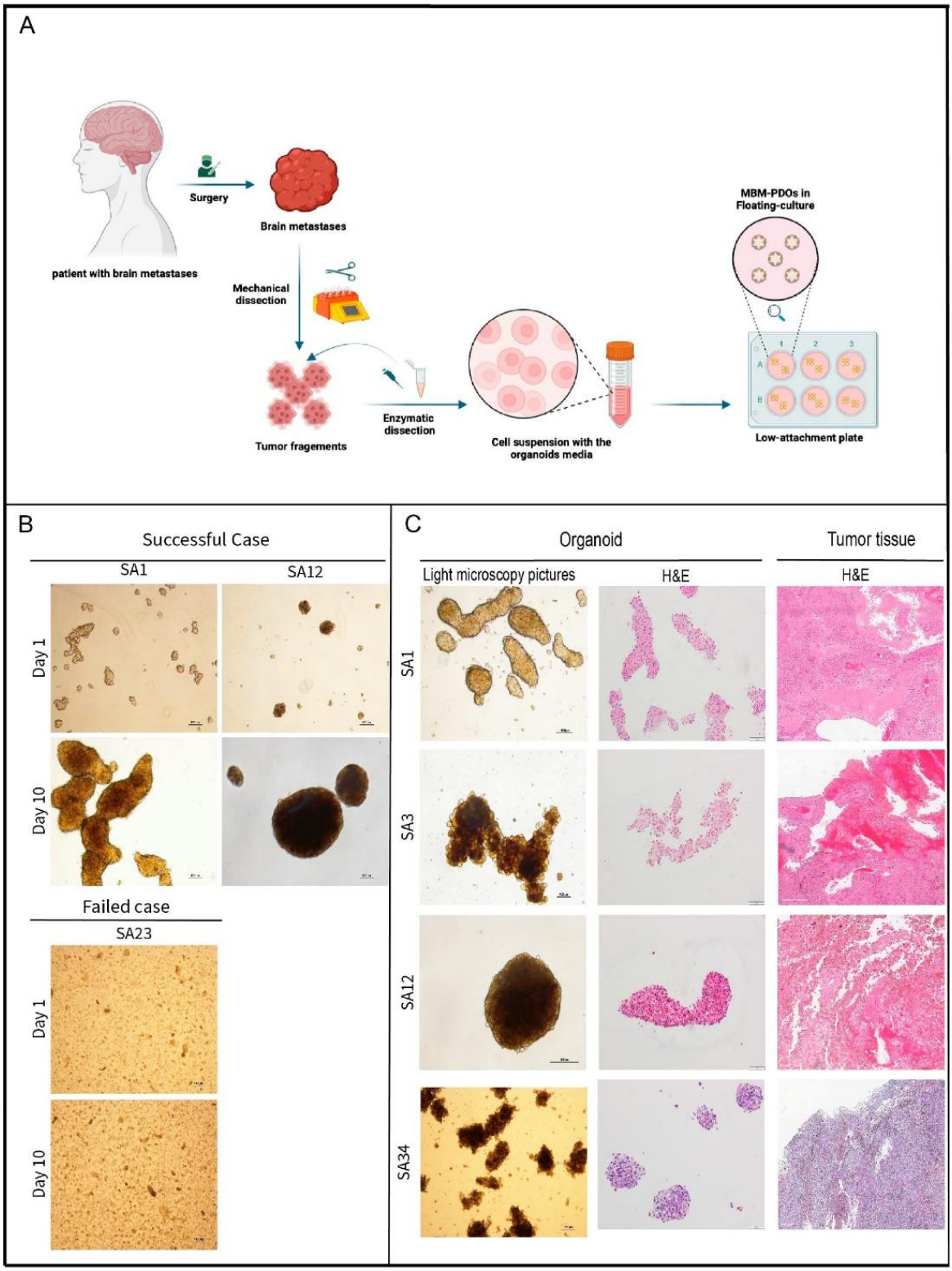

Figure 1. (**A**) Graphical representation for the MBM-PDOs' generation workflow. Tumor samples are dissociated into single-cell suspensions and grown in low-attachment plates (created with BioRender.com). (**B**) Bright-field images of PDOs after 1 day and 10 days of culture establishment (scale bar 100 µm). (**C**) Bright-field images (5× magnification) and hematoxylin and eosin (H&E) staining (10× magnification) showing different phenotypes of MBM-PDOs.

The growth rate of the MBM-PDOs was visualized 2–3 times per week using a bright-field microscope. A variability in the growth rate was observed among the MBM-PDO cultures. Some cultures expanded exponentially within 10–14 days, after which a growth plateau was reached. Other cultures proliferated at a slower rate (the growth plateau was reached in 20–25 days). Therefore, the MBM-PDOs with a high rate of proliferation required passaging every 10–14 days, whereas the slower-proliferating organoids were re-passaged every 20–25 days. We further evaluated the organoids' rate of growth by employing Ki-67 staining and distinguished them as having either a low or a high proliferation rate ($\leq$ or >40% of Ki-67 positive nuclei, respectively) (Supplementary Table S2). Five of the organoid cultures exhibited a high proliferation rate, while the remaining two organoid cultures displayed a low proliferation rate, and these distinctions were observed across different days.

4.2. MBM-PDOs Preserve Key Histological Features of Their Original Tumors

We could cultivate the organoids over a median of eight passages (range four to twelve passages) and the histological features of the MBM-PDOs remained stable over the passages.

To confirm that the PDOs faithfully recapitulated the histomorphology and histological features observed in the original tumors, we conducted a comparative immunohistochemical (IHC) staining. The cultivated MBM-PDOs exhibited positivity for melanoma markers, including S100, Melan A, and HMB45, consistent with their expression in the parental tumor samples (Figure 2).

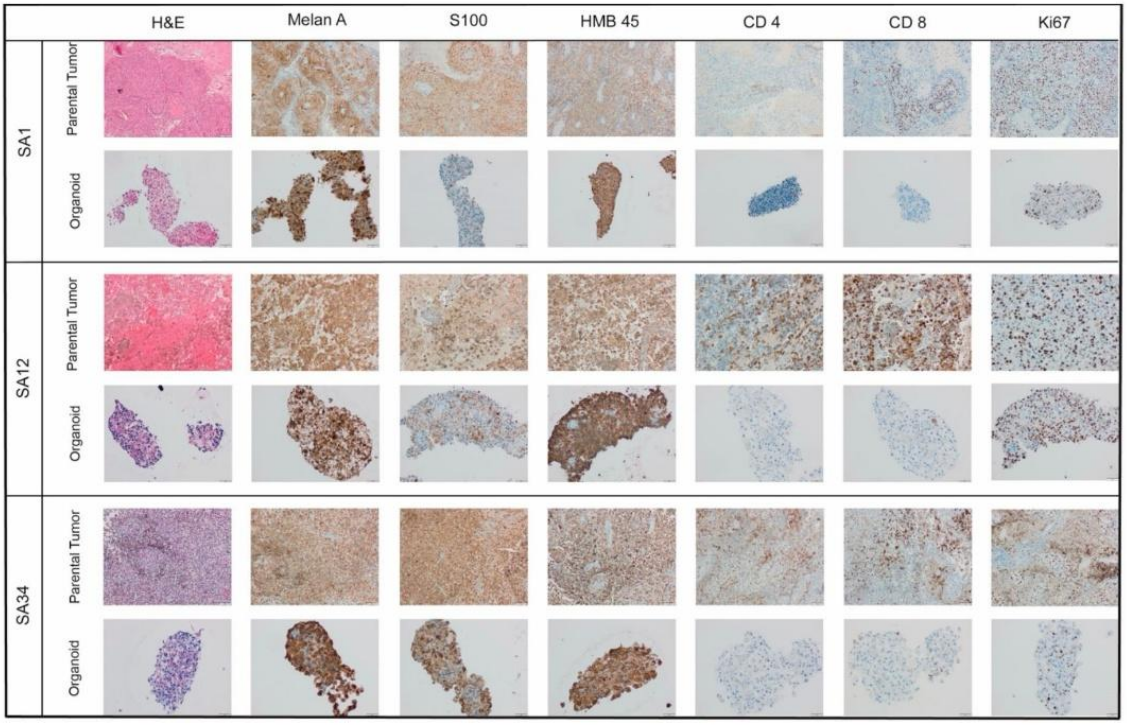

Figure 2. Representative images of hematoxylin and eosin (H&E) staining and immunohistochemical staining (for Melan A, S100, HMB45, CD4, CD8, and Ki67) of the parental tumors and their MBM-PDO cultures (10× and 20× magnification).

However, it is noteworthy that the PDO cultures did not preserve the tumor immune microenvironment, resulting in negative stainings for CD4 and CD8 (Figure 2).

Importantly, the PDO cultures displayed stability in their melanoma immunohistochemistry markers, maintaining positive staining for S100 and Melan A even after multiple passages (Figure 3A,B).

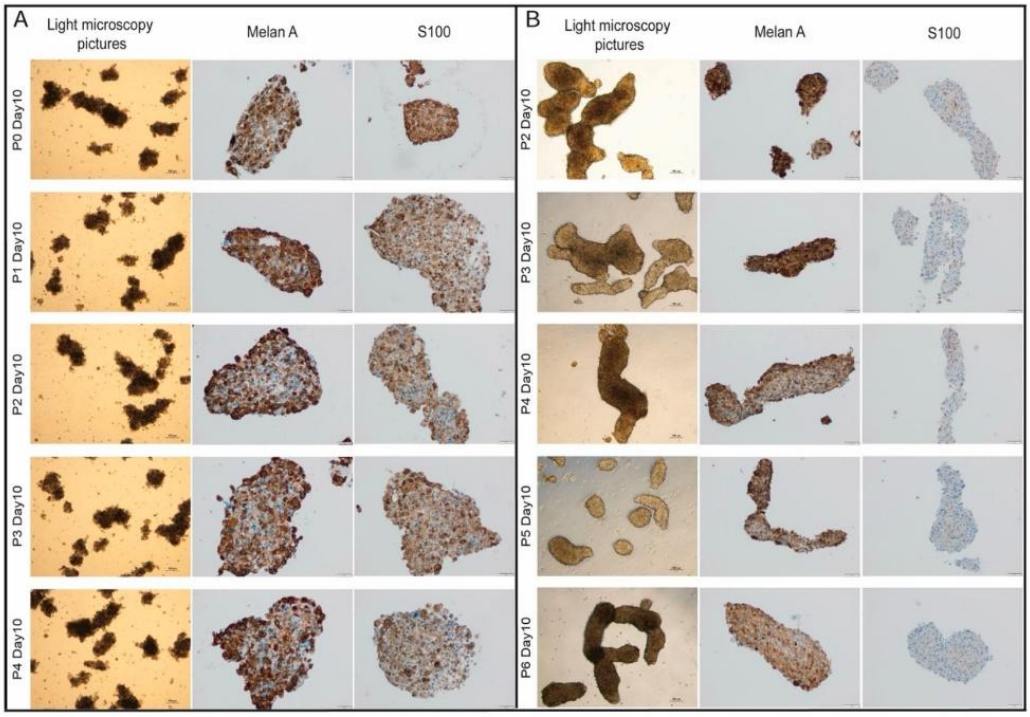

Figure 3. Bright-field images (5× magnification) and representative images of immunohistochemical stainings for Melan A and S100 staining (10× magnification) of different passages showing the stability of organoid-morphology and immunohistochemical profile. (**A**) SA34 MBM-PDO culture. (**B**) SA1 MBM-PDO culture. P, passage.

4.3. MBM-PDOs Recapitulate the Mutational Profiles of Their Original Tumors

Five out of the seven melanoma brain metastases harbored the *BRAF* V600E mutation, and two out of the seven cases had other less frequent mutations (one *NRAS* mutation, one *KIT* mutation). Those two cases were exposed to a panel next-generation sequencing to test for further mutations. Five out of the seven MBM-PDO cultures fully maintained the mutational profile of the parental brain metastasis tissue. One case with *BRAF* wild type lost in vitro the *POLE* mutation demonstrated in the parental tumor (Table 2). In addition, one MBM-PDO culture acquired a *TERT* mutation that was not found in the parental tumor.

Table 2. Mutational analysis of the primary tumors and paired PDO.

Case	Primary Tumor	Organoid
SA1	*BRAF V600 E*	*BRAF V600 E*
SA3	*BRAF V600 E*	*BRAF V600 E*
SA12	*BRAF V600 E*	*BRAF V600 E*
SA17	*BRAF V600 E*	*BRAF V600 E*
SA20	*BRAF V600 E*	*BRAF V600 E*
SA34	*BRAF V600 WT*	*BRAF V600 WT*
	NRAS p.Q61K	*NRAS p.Q61K*
		TERT c.146C>T
SA41	*BRAF V600 WT*	*BRAF V600 WT*
	KIT p.L576P	*KIT p.L576P.*
	TERT c.146C>T	*TERT c.146C>T*
	TERT c.125_124delinsTT	*TERT c.125_124delinsTT*
	POLE c.1360-1>A	

4.4. MBM-PDOs with BRAF V600E Mutations Show Therapy Response to BRAF and MEK Inhibitors

The MBM-PDO cultures were treated with a combination of dabrafenib (*BRAF* inhibitor) and trametinib (*MEK* inhibitor) at four different concentrations (1 µM + 1 µM, 0.5 µM + 0.5 µM, 0.25 µM + 0.25 µM, 0.125 µM + 0.125 µM) for three days, followed by a cell viability assessment (Figure 4A). The efficacy of the *BRAF* and *MEK* inhibitors on the responding PDO cultures was visually apparent through morphological changes in the organoids (Figure 4C). MBM-PDO cultures with the *BRAF* V600E mutation exhibited good therapy responses to the targeted therapy involving the *BRAF* and *MEK* inhibitors, resulting in marked reductions in cell viability (<50%), whereas the *BRAF* wild-type cultures showed no changes in cell viability (Figure 4B). All four cases treated with *BRAF* and *MEK* inhibitors had a high proliferation rate (Ki-67 > 40%) (Supplementary Table S2).

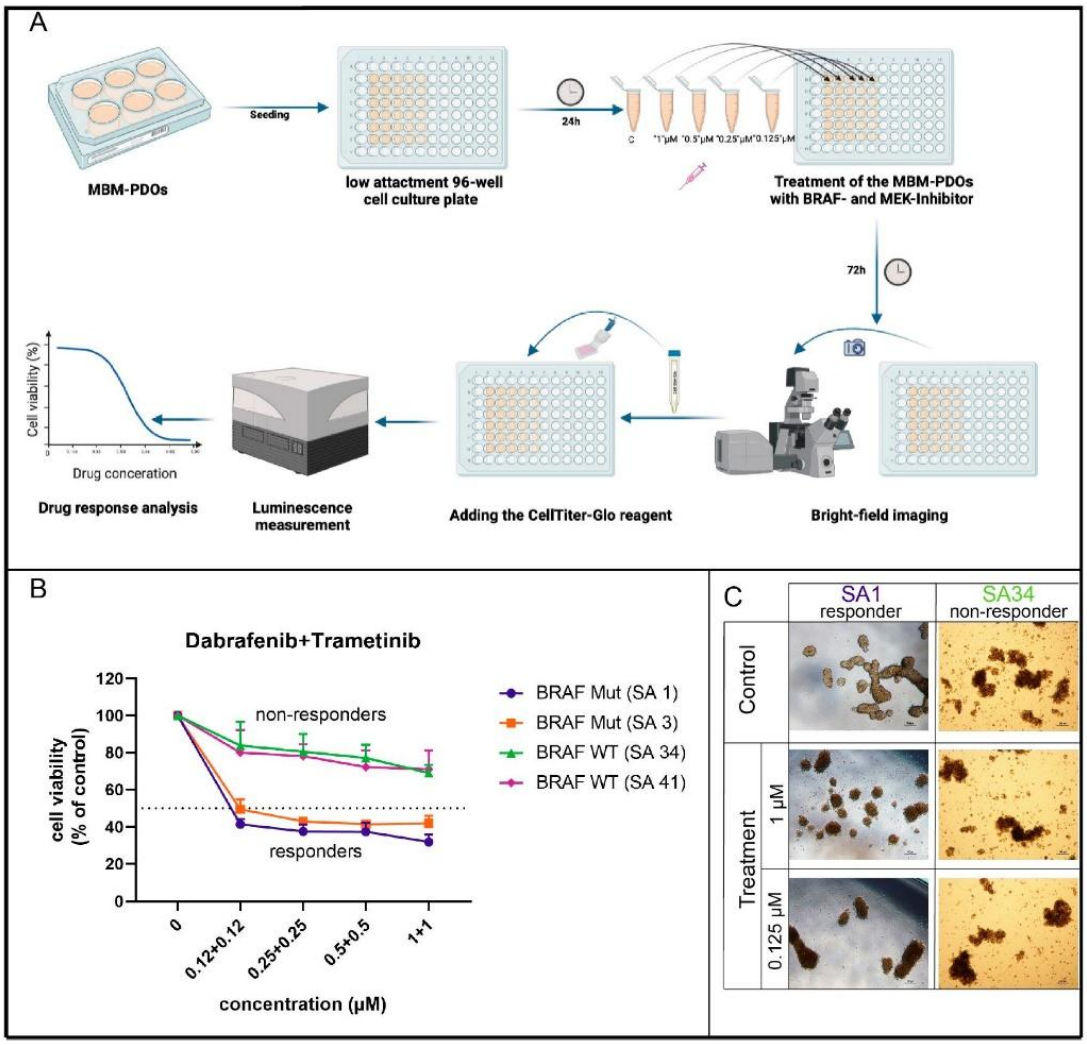

Figure 4. (**A**) Graphical abstract for the in vitro drug sensitivity assay (created with Biorender.com). (**B**) A dose–response graph depicting the cell viability of MBM-PDO cultures treated with different concentrations of dabrafenib and trametinib for 72 h. Cell viability, assessed using the CellTiter-Glo assay (Promega), was normalized to the vehicle control. Each condition was tested in technical and biological triplicates. Data are presented as mean ± SEM. (**C**) Representative brightfield microscopy images of MBM-PDO cultures taken after 72 h of treatment with 1 µM and 0.125 µM dabrafenib and trametinib, as well as vehicle control (top row) (scale bar 100 µm).

5. Discussion

Patient-derived models, such as organoids and tumoroids, are important tools for studying tumor biology and for testing newly developed treatment modalities [13–16]. Recently, Sun et al. (2023) [17] described organoids derived from primary mucosal melanomas. These organoids retained the histological and molecular features of the primary tumors and could be utilized for assessing drug therapy responses. Currently, limited data about organoid generation from primary skin melanoma are available [18,19].

To our knowledge, this is the first study establishing organoids from melanoma brain metastases. We were able to successfully cultivate seven out of eight cases for up to 10 passages. The one case that failed to grow was a brain metastasis relapse, which recurred following surgical resection of a melanoma brain metastasis, followed by stereotactic radiotherapy and immune checkpoint inhibitor therapy. This may be due to the prior therapy and the fact that we tried to cultivate tissue from a relapsed metastasis. The MBM-PDO cultures were stable in culture for several passages, preserving the histological phenotype of the parental tumors throughout the passages, which is in line with the observations of Sun et al. in mucosal melanoma organoids (Sun et al., 2023) [17]. The inter-patient variation in the morphology of the MBM-PDOs could be associated with genetic heterogeneity, differences in the tumor microenvironment, and variations in cellular composition among the patients' tumors [20]. The MBM-PDO cultures exhibited varying proliferative activities, as revealed by Ki-67 staining. Some MBM-PDO cultures were highly proliferative (>40% positive nuclei), while others were lowly proliferative (<40%). The proliferation rate was concordant between the MBM-PDOs and their parental tumors. The absence of a tumor immune microenvironment in the generated MBM-PDO culture limits the model's ability to accurately recapitulate tumor–immune interactions. To address this limitation, several strategies can be employed in the future such as autologous or allogeneic immune cells and organoid co-culture systems [21]. Additionally, the inclusion of specific cytokines and growth factors, such as interleukin-2 (IL-2), can enhance the viability and proliferation of immune cells within the organoids, thereby improving the recapitulation of the in vivo microenvironment [22]. We assessed the mutational status of the parental brain metastasis tissue and the MBM-PDO cultures and observed that *BRAF* mutations were conserved in culture. Five out of seven MBM-PDO cultures (71%) fully recapitulated the mutational profile of their parental tumors. Notably, both MBM-PDO cultures from *BRAF* wild-type melanomas also had *TERT* promoter mutations. *TERT* mutations are common in melanoma (69%) and are associated with a poor prognosis [23]. The most frequent mutation in primary brain tumors as well as in metastasis is the *C250T* mutation, corresponding to the mutation observed in our two cases. Interestingly, Blanco-Garcia et al. [23] also noticed that the *C250T TERT* mutation was often associated with *NRAS* mutations, which was detected in one of our two cases with a *TERT* mutation. To demonstrate the close molecular similarity between the MBM-PDOs and their parental tissue, transcriptomic profiles from the MBM-PDOs as well as their parental tissue could be analyzed via bulk RNA sequencing. Melanoma brain metastases are the primary cause of death in 60–70% of melanoma cases [24]. Since the introduction of tyrosine kinase inhibitors and the MAPK inhibitors for the treatment of metastatic melanomas, the overall survival of patients increased dramatically. Two clinical studies, COMBI-d and COMBI-v, conducted on patients with metastasized melanoma and *BRAF* V600E and *V600K* mutations, showed a 5-year overall survival rate of 34% and a median overall survival time of 25.9 months with dabrafenib plus trametinib treatment [25]. For melanoma brain metastases with *BRAF V600* mutations, a combination therapy with dabrafenib and trametinib is effective; however, the responses are less durable than those of extracranial metastases with the same mutations [26]. The COMBI-r study reported a 10.8 months overall survival for patients with melanoma brain metastases with *BRAF V600E* or *V600K* mutations treated with dabrafenib/trametinib as the first-line therapy [27]. We aimed to test the feasibility of utilizing MBM-PDO cultures as an in vitro platform to identify the efficacy of targeted therapy. To that end, we treated four cultures with a combination of

dabrafenib/trametinib. As expected and described by Sun et al., the treatment response correlated with the mutational status of the tumors [17]. Two MBM-PDO cultures harboring *BRAF* V600E mutations had a very good response to the combination therapy, as assessed by cell viability, while the *BRAF* wild-type cultures were insensitive. Interestingly, the MBM-PDOs harboring an *NRAS* mutation were also insensitive to therapy. Since we treated the PDOs with *MEK* inhibitors, besides *BRAF* inhibitors, we expected a therapy response, even if it was not as pronounced as for PDOs with *BRAF* mutations. This underlines the individualized patients' response to targeted therapy.

In conclusion, we successfully established patient-derived organoids from melanoma brain metastases, which faithfully recapitulated the histological and mutational characteristics in culture, over passages. In vitro drug testing demonstrated the capacity of the MBM-PDOs to reveal targeted-therapy susceptibilities, which highlights their great potential in preclinical research, drug discovery, and personalized medicine.

Supplementary Materials: The following supporting information can be downloaded at https://www.mdpi.com/article/10.3390/pharmaceutics16081042/s1, Table S1: MBM-PDO culture media; Table S2: Quantification of Ki67 staining.

Author Contributions: Study concept and design: M.I.T., S.-E.A., M.H. (Michael Hölzel), and E.G. Acquisition of data: S.-E.A., R.H., A.W., and G.H.G. Analysis and interpretation of data: all coauthors. Drafting of the manuscript: S.-E.A., M.I.T., R.H., J.S., A.F., G.H.G., A.W., and M.S. Critical revision of the manuscript for important intellectual content: all coauthors. All authors have read and agreed to the published version of the manuscript.

Funding: S.-E.A. and this study were partially supported by the Bonfor internal funding program of the Medical Faculty Bonn. A.F. is funded by the Deutsche Krebshilfe through a Mildred Scheel Nachwuchszentrum Grant (Grant number 70113307).

Institutional Review Board Statement: This study was performed according with the Declaration of Helsinki. Informed consent was obtained from all patients included. This study was approved by the Ethics Committee of the Medical Faculty, University Bonn (#417/17 with amendment from 2020; #169/23).

Informed Consent Statement: Informed consent was obtained from all subjects involved in the study. However, written informed consent for publication was not obtained because the patients who participated in the study were deceased by the time the study was terminated.

Data Availability Statement: The datasets analyzed during the current study are available from the corresponding author on reasonable request.

Acknowledgments: The authors thank Susanne Steiner, Agnes Leier, and Carsten Golletz for their excellent technical assistance. We are also grateful to Frigga Hönig who helped us with the sample logistics. We thank the staff of the Institute of Pathology, the Institute of Neuropathology, and the medical staff of the Clinic for Neurosurgery for their support.

Conflicts of Interest: The authors have no competing interests regarding this study.

Abbreviations

PDO	patient-derived organoid
MBM	melanoma brain metastasis
MBM-PDO	patient-derived organoid from melanoma brain metastases
NGS	next-generation sequencing

References

1. Achrol, A.S.; Rennert, R.C.; Anders, C.; Soffietti, R.; Ahluwalia, M.S.; Nayak, L.; Peters, S.; Arvold, N.D.; Harsh, G.R.; Steeg, P.S.; et al. Brain metastases. *Nat. Rev. Dis. Primer* **2019**, *5*, 5. [CrossRef] [PubMed]
2. Nayak, L.; Lee, E.Q.; Wen, P.Y. Epidemiology of brain metastases. *Curr. Oncol. Rep.* **2012**, *14*, 48–54. [CrossRef] [PubMed]

3. Stelzer, K.J. Epidemiology and prognosis of brain metastases. *Surg. Neurol. Int.* **2013**, *4* (Suppl. S4), S192–S202. [CrossRef] [PubMed]
4. Davies, H.; Bignell, G.R.; Cox, C.; Stephens, P.; Edkins, S.; Clegg, S.; Teague, J.; Woffendin, H.; Garnett, M.J.; Bottomley, W.; et al. Mutations of the BRAF gene in human cancer. *Nature* **2002**, *417*, 949–954. [CrossRef] [PubMed]
5. Robert, C.; Karaszewska, B.; Schachter, J.; Rutkowski, P.; Mackiewicz, A.; Stroiakovski, D.; Lichinitser, M.; Dummer, R.; Grange, F.; Mortier, L.; et al. Improved overall survival in melanoma with combined dabrafenib and trametinib. *N. Engl. J. Med.* **2015**, *372*, 30–39. [CrossRef] [PubMed]
6. Ascierto, P.A.; McArthur, G.A.; Dréno, B.; Atkinson, V.; Liszkay, G.; Di Giacomo, A.M.; Mandala, M.; Demidov, L.; Stroyakovskiy, D.; Thomas, L.; et al. Cobimetinib combined with vemurafenib in advanced BRAF(V600)-mutant melanoma (coBRIM): Updated efficacy results from a randomised, double-blind, phase 3 trial. *Lancet Oncol.* **2016**, *17*, 1248–1260. [CrossRef] [PubMed]
7. Larkin, J.; Chiarion-Sileni, V.; Gonzalez, R.; Grob, J.J.; Rutkowski, P.; Lao, C.D.; Cowey, C.L.; Schadendorf, D.; Wagstaff, J.; Dummer, R.; et al. Five-Year Survival with Combined Nivolumab and Ipilimumab in Advanced Melanoma. *N. Engl. J. Med.* **2019**, *381*, 1535–1546. [CrossRef] [PubMed]
8. Robert, C.; Ribas, A.; Schachter, J.; Arance, A.; Grob, J.J.; Mortier, L.; Daud, A.; Carlino, M.S.; McNeil, C.M.; Lotem, M.; et al. Pembrolizumab versus ipilimumab in advanced melanoma (KEYNOTE-006): Post-hoc 5-year results from an open-label, multicentre, randomised, controlled, phase 3 study. *Lancet Oncol.* **2019**, *20*, 1239–1251. [CrossRef] [PubMed]
9. Robert, C.; Carlino, M.S.; McNeil, C.; Ribas, A.; Grob, J.J.; Schachter, J.; Nyakas, M.; Kee, D.; Petrella, T.M.; Blaustein, A.; et al. Seven-Year Follow-Up of the Phase III KEYNOTE-006 Study: Pembrolizumab Versus Ipilimumab in Advanced Melanoma. *J. Clin. Oncol. Off. J. Am. Soc. Clin. Oncol.* **2023**, *41*, 3998–4003. [CrossRef]
10. Kim, M.; Mun, H.; Sung, C.O.; Cho, E.J.; Jeon, H.J.; Chun, S.M.; Jung, D.J.; Shin, T.H.; Jeong, G.S.; Kim, D.K.; et al. Patient-derived lung cancer organoids as in vitro cancer models for therapeutic screening. *Nat. Commun.* **2019**, *10*, 3991. [CrossRef]
11. Karkampouna, S.; La Manna, F.; Benjak, A.; Kiener, M.; De Menna, M.; Zoni, E.; Grosjean, J.; Klima, I.; Garofoli, A.; Bolis, M.; et al. Patient-derived xenografts and organoids model therapy response in prostate cancer. *Nat. Commun.* **2021**, *12*, 1117. [CrossRef] [PubMed]
12. Wensink, G.E.; Elias, S.G.; Mullenders, J.; Koopman, M.; Boj, S.F.; Kranenburg, O.W.; Roodhart, J.M.L. Patient-derived organoids as a predictive biomarker for treatment response in cancer patients. *NPJ Precis. Oncol.* **2021**, *5*, 30. [CrossRef] [PubMed]
13. Freitas de Morais, E.; Siquara da Rocha, L.d.O.; de Souza Santos, J.L.; Freitas, R.D.; Souza, B.S.d.F.; Coletta, R.D.; Gurgel Rocha, C.A. Use of Three-Dimensional Cell Culture Models in Drug Assays for Anti-Cancer Agents in Oral Cancer: Protocol for a Scoping Review. *J. Pers. Med.* **2023**, *13*, 1618. [CrossRef] [PubMed]
14. Sahgal, P.; Patil, D.T.; Bala, P.; Sztupinszki, Z.M.; Tisza, V.; Spisak, S.; Luong, A.G.; Huffman, B.; Prosz, A.; Singh, H.; et al. Replicative stress in gastroesophageal cancer is associated with chromosomal instability and sensitivity to DNA damage response inhibitors. *iScience* **2023**, *26*, 108169. [CrossRef] [PubMed]
15. Vazquez-Armendariz, A.I.; Tata, P.R. Recent advances in lung organoid development and applications in disease modeling. *J. Clin. Investig.* **2023**, *133*, e170500. [CrossRef] [PubMed]
16. Ren, X.; Huang, M.; Weng, W.; Xie, Y.; Wu, Y.; Zhu, S.; Zhang, Y.; Li, D.; Lai, J.; Shen, S.; et al. Personalized drug screening in patient-derived organoids of biliary tract cancer and its clinical application. *Cell Rep. Med.* **2023**, *4*, 101277. [CrossRef] [PubMed]
17. Sun, L.; Kang, X.; Ju, H.; Wang, C.; Yang, G.; Wang, R.; Sun, S. A human mucosal melanoma organoid platform for modeling tumor heterogeneity and exploring immunotherapy combination options. *Sci. Adv.* **2023**, *9*, eadg6686. [CrossRef] [PubMed]
18. Ou, L.; Liu, S.; Wang, H.; Guo, Y.; Guan, L.; Shen, L.; Luo, R.; Elder, D.E.; Huang, A.C.; Karakousis, G.; et al. Patient-derived melanoma organoid models facilitate the assessment of immunotherapies. *EBioMedicine* **2023**, *92*, 104614. [CrossRef] [PubMed]
19. Zhou, S.; Lu, J.; Liu, S.; Shao, J.; Liu, Z.; Li, J.; Xiao, W. Role of the tumor microenvironment in malignant melanoma organoids during the development and metastasis of tumors. *Front. Cell Dev. Biol.* **2023**, *11*, 1166916. [CrossRef]
20. Tiriac, H.; Belleau, P.; Engle, D.D.; Plenker, D.; Deschênes, A.; Somerville, T.D.D.; Froeling, F.E.M.; Burkhart, R.A.; Denroche, R.E.; Jang, G.-H.; et al. Organoid Profiling Identifies Common Responders to Chemotherapy in Pancreatic Cancer. *Cancer Discov.* **2018**, *8*, 1112–1129. [CrossRef]
21. Yuan, J.; Li, X.; Yu, S. Cancer organoid co-culture model system: Novel approach to guide precision medicine. *Front. Immunol.* **2022**, *13*, 1061388. [CrossRef] [PubMed]
22. Neal, J.T.; Li, X.; Zhu, J.; Giangarra, V.; Grzeskowiak, C.L.; Ju, J.; Liu, I.H.; Chiou, S.-H.; Salahudeen, A.A.; Smith, A.R.; et al. Organoid Modeling of the Tumor Immune Microenvironment. *Cell* **2018**, *175*, 1972–1988.e16. [CrossRef] [PubMed]
23. Blanco-García, L.; Ruano, Y.; Blanco Martínez-Illescas, R.; Cubo, R.; Jiménez Sánchez, P.; Sánchez-Arévalo Lobo, V.J.; Falkenbach, E.R.; Romero, P.O.; Garrido, M.C.; Peralto, J.L.R.; et al. pTERT C250T mutation: A potential biomarker of poor prognosis in metastatic melanoma. *Heliyon* **2023**, *9*, e18953. [CrossRef] [PubMed]
24. Gutzmer, R.; Vordermark, D.; Hassel, J.C.; Krex, D.; Wendl, C.; Schadendorf, D.; Sickmann, T.; Rieken, S.; Pukrop, T.; Höller, C.; et al. Melanoma brain metastases-Interdisciplinary management recommendations 2020. *Cancer Treat. Rev.* **2020**, *89*, 102083. [CrossRef] [PubMed]
25. Robert, C.; Grob, J.J.; Stroyakovskiy, D.; Karaszewska, B.; Hauschild, A.; Levchenko, E.; Chiarion Sileni, V.; Schachter, J.; Garbe, C.; Bondarenko, I.; et al. Five-Year Outcomes with Dabrafenib plus Trametinib in Metastatic Melanoma. *N. Engl. J. Med.* **2019**, *381*, 626–636. [CrossRef] [PubMed]

26. Davies, M.A.; Saiag, P.; Robert, C.; Grob, J.J.; Flaherty, K.T.; Arance, A.; Chiarion Sileni, V.; Thomas, L.; Lesimple, T.; Mortier, L.; et al. Dabrafenib plus trametinib in patients with BRAFV600-mutant melanoma brain metastases (COMBI-MB): A multicentre, multicohort, open-label, phase 2 trial. *Lancet Oncol.* **2017**, *18*, 863–873. [CrossRef]
27. Berking, C.; Livingstone, E.; Debus, D.; Loquai, C.; Weichenthal, M.; Leiter, U.; Kiecker, F.; Mohr, P.; Eigentler, T.K.; Remy, J.; et al. COMBI-r: A Prospective, Non-Interventional Study of Dabrafenib Plus Trametinib in Unselected Patients with Unresectable or Metastatic BRAF V600-Mutant Melanoma. *Cancers* **2023**, *15*, 4436. [CrossRef]

3.3 Publications 3: Expression of the large amino acid transporter SLC7A5/LAT1 on immune cells is enhanced in primary sclerosing cholangitis-associated cholangiocarcinoma and correlates with poor prognosis in cholangiocarcinoma / DOI: https://doi.org/10.1016/j.humpath.2024.105670

Human Pathology 153 (2024) 105670

Contents lists available at ScienceDirect

Human Pathology

journal homepage: www.elsevier.com/locate/humpath

Expression of the large amino acid transporter SLC7A5/LAT1 on immune cells is enhanced in primary sclerosing cholangitis-associated cholangiocarcinoma and correlates with poor prognosis in cholangiocarcinoma

Vittorio Branchi [a,1], Racha Hosni [b,1], Lukas Kiwitz [e], Susanna Ng [e], Gemma van der Voort [e], Neila Bambi [b], Eileen Kleinfelder [b], Laura K. Esser [b], Leona Dold [c], Bettina Langhans [c], Maria A. Gonzalez-Carmona [c], Saskia Ting [d,2], Glen Kristiansen [b], Jörg C. Kalff [a], Kevin Thurley [e], Michael Hölzel [e], Hanno Matthaei [a], Marieta I. Toma [b,*]

[a] Department of General, Abdominal, Thoracic and Vascular Surgery, University Hospital Bonn, Venusberg-Campus 1, 53127, Bonn, Germany
[b] Institute of Pathology, University Hospital Bonn, Venusberg-Campus 1, 53127, Bonn, Germany
[c] Department of Internal Medicine I, University Hospital Bonn, Venusberg-Campus 1, 53127, Bonn, Germany
[d] Institute of Pathology, University Hospital Essen, Hufelandstr. 55, 45147, Essen, Germany
[e] Institute of Experimental Oncology, University Hospital Bonn, Venusberg-Campus 1, 53127, Bonn, Germany

ARTICLE INFO

Keywords:
Biliary tract cancer
Cholangiocellular carcinoma
Primary sclerosing cholangitis
SLC7A5

ABSTRACT

Biliary tract cancers (BTC) are rare lethal malignancies arising along the biliary tree. Unfortunately, effective therapeutics are lacking and the prognosis remains dismal even for patients eligible for surgical resection. Therefore, novel therapeutic approaches along with early detection strategies and prognostic markers are urgently needed. Primary sclerosing cholangitis (PSC) is a chronic disease of the bile ducts leading to fibrosis and ultimately cirrhosis. Patients with PSC have a 5–20% lifetime risk of developing BTC; yet the molecular mechanisms that underpin the development of PSC- associated biliary tract cancer (PSC-BTC) have not been fully elucidated. SLC7A5/LAT1, a large amino acid transporter, has been shown to modulate cell growth and proliferation as well as other intracellular processes in solid tumors. In this study, we evaluated *SLC7A5* expression in PSC-BTC and in sporadic BTC (sBTC) and its role as a prognostic factor. Analysis of the TGCA cohort showed a significantly higher expression of *SLC7A5* in tumor tissue compared with adjacent normal tissue ($p = 0.0002$) in BTC. In our cohort (comprised of 69 BTC patients including 16 PSC-BTC), SLC7A5/LAT1 expression was observed in both tumor and intratumoral immune cells. A significantly higher percentage of SLC7A5/LAT1 positive intratumoral immune cells was observed in PSC-BTC compared with sBTC ($p = 0.004$). Multiplex immunofluorescence co-detection by indexing (CODEX) analysis identified $CD4^+$ regulatory T lymphocytes and $CD68^+$ macrophages as the largest immune cell populations expressing LAT1.

SLC7A5/LAT1 expression as well as a higher intratumoral infiltration of SLC7A5/LAT1-positive immune cells (≥2%) were associated with a shorter overall survival in our cohort (LogRank test, $p = 0.04$ and $p = 0.008$; respectively). SLC7A5/LAT1 expressing tumors are higher staged tumors (pT3/4 versus pT1/2, $p = 0.048$).

Abbreviations: BTC, biliary tract cancer; sBTC, sporadic biliary tract cancer; PSC, primary sclerosing cholangitis; PSC-BTC, primary sclerosing cholangitis-associated biliary tract cancer; pCCA, perihilar cholangiocarcinoma; dCCA, distal cholangiocarcinoma; iCCA, intrahepatic cholangiocarcinoma; GBC, gallbladder cancer; OS, overall survival; DFS, disease-free survival; TMA, tissue microarray; TCGA, The Cancer Genome Atlas.

* Corresponding author.
E-mail addresses: Vittorio.Branchi@ukbonn.de (V. Branchi), Racha.Hosni@ukbonn.de (R. Hosni), Leona.Dold@ukbonn.de (L. Dold), Bettina.Langhans@ukbonn.de (B. Langhans), Maria.Gonzalez@ukbonn.de (M.A. Gonzalez-Carmona), ting@patho-nordhessen.de (S. Ting), Glen.Kristiansen@ukbonn.de (G. Kristiansen), kalff@uni-bonn.de (J.C. Kalff), mholzel@uni-bonn.de (M. Hölzel), Hanno.Matthaei@ukbonn.de (H. Matthaei), Marieta.Toma@ukbonn.de (M.I. Toma).
[1] Equal contribution.
[2] Current address. Institute of Pathology Nordhessen, Kassel, Germany.

https://doi.org/10.1016/j.humpath.2024.105670
Received 25 July 2024; Received in revised form 25 September 2024; Accepted 30 September 2024
Available online 13 October 2024

These results underline the potential use of SLC7A5/LAT1 as a prognostic marker in BTC. Furthermore, the higher frequency of SLC7A5/LAT1 positive immune cells in PSC-BTC compared to sBTC may hint at the potential role of SLC7A5/LAT1 in inflammation-driven carcinogenesis.

1. Introduction

Biliary tract cancers (BTCs) are rare, aggressive tumors arising from the epithelium of the biliary tract. BTCs include intrahepatic cholangiocarcinoma (iCCA) and extrahepatic cholangiocarcinoma, the latter comprising perihilar cholangiocarcinoma (pCCA) and distal cholagiocarcinoma (dCCA), as well as gallbladder cancers (GBCs).

Four histological subtypes associated with BTC localization and specific mutations have been described: small bile duct, large bile duct, mucinous, and papillary. Extrahepatic CCAs (pCCAs and dCCAs) are mostly conventional mucin-producing adenocarcinomas or papillary tumors [1].

iCCAs are further classified according to the affected bile ducts into small and large bile duct types. Small duct iCCAs are characterized by proliferations of small ducts, tubuli or acini with a nodular growth pattern, with sparse or no mucin production. Large duct iCCAs arise in large intrahepatic bile ducts and present a macroacinary or papillary architecture of mucin-producing columnar cells [2]. Interestingly, the histological phenotype seems to be driven by molecular heterogeneity. Small duct iCCAs often have *IDH1* and *IDH2* mutations, as well as *FGFR2* gene fusions, while large duct iCCA are similar to the extrahepatic CCA; often harboring *TP53* and *KRAS* mutations [3–9]. The incidence of intra- and extrahepatic BTCs has been significantly increasing during the past few years, whereas GBC incidence has been decreasing over the past decades [10]. Most individuals with BTC receive diagnosis at an advanced, unresectable stage, primarily because symptoms are typically absent during the initial phases of the disease [11,12]. Therefore, only about 25% of patients with BTC can undergo a surgical resection. Even after surgical resection, the median overall survival (OS) ranges from 8 to 16 months [13].

The standard treatment for advanced BTC (gemcitabine plus cisplatin) has remained consistent for over a decade. Durvalumab, a checkpoint inhibitor targeting PD-L1, was recently found to increase overall survival in this group of patients [14,15].

Risk factors for BTCs are related to chronic inflammation and include liver flukes, viral hepatitis, cholelithiasis, and primary sclerosing cholangitis (PSC) [16]. PSC is a rare disease with an unclear etiology and is often linked with inflammatory bowel diseases. PSC is a chronic condition affecting the bile ducts characterized by periductal concentric fibrosis. These fibrotic changes lead to duct fibrotic strictures, cholestasis and liver cirrhosis [17]. Although the pathogenesis of PSC-associated BTC (PSC-BTC) has not been completely elucidated, it is believed that genetic, inflammatory, immunological, and physical factors play an important role. PSC patients have an increased production and excretion of biliary IL-6 and increased expression of senescence markers like p16 and γH2A.x [18]. Sustained increased IL-6-STAT3 signaling leads to MCL1 (myeloid leukemia 1) upregulation, increased mitogenesis, as well as activation of nitric oxide synthase leading to excess of nitric oxide and subsequent DNA damage [19,20]. PSC-BTCs harbor genomic alterations typical for extrahepatic sBTC, namely mutations in *TP53, KRAS, CDKN2A, PIK3CA, GNAS1 or SMAD4* [21,22]. DNA copy number variations seem to be an early event in PSC-associated carcinogenesis, whereas gene mutations occur later in the development of PSC-BTC [22].

SLC7A5 encodes a large amino-acid transporter, which is responsible for the cellular uptake of amino acids, especially large neutral amino acids, such as L-leucine [23]. SLC7A5 (also known as LAT1) modulates cell growth, cell proliferation as well as other intracellular processes in tumors such as glioblastoma, and plays an important role in the metastatic pathways of several solid tumors including colorectal carcinomas [24]. Recently published research on BTC demonstrated that a high expression of SLC7A5/LAT1 in tumor cells is correlated with poor prognosis, and inhibition of SLC7A5/LAT1 improves the response to chemotherapy *in vitro* [25–27]. A high SLC7A5/LAT1 expression was associated with poor survival and increased expression of proliferation and hypoxia-related genes in estrogen receptor-positive breast cancer [28,29]. In addition, SLC7A5/LAT1 regulates the activation status of several immune cells in the peripheral immune system and a high expression was also associated with intratumoral T-helper cells and NK cells in breast cancer [28,30]. SLC7A5/LAT1 is highly abundant in primary central nervous system tumors as well as at the blood-brain barrier, making it a reliable target for drug delivery in the central nervous system tumors [31]. In solid cancers, a first phase I trial has reported disease control or partial response in two of five treated biliary tract cancer patients [32]. This provides a rationale for testing combination therapies of LAT1/SLC7A5 inhibitors with standard chemotherapy, which may potentially lead to prolonged patients' survival.

The objective of this study was to compare the expression of SLC7A5/LAT1 between PSC-BTC and sBTC, with a particular focus on evaluating its expression within the immune microenvironment and its potential as a prognostic factor in BTC.

2. Material and methods

2.1. Patients and samples

For immunohistochemical analysis, tumor samples from a cohort of patients who underwent surgical resection for malignant tumors of the biliary tract between 2013 and 2017 at the Department of Surgery, University Hospital Bonn were analyzed. Patients' data including pathological stage, grading, sex, age and adjuvant therapy were collected (Table 1). Four patients presented with inoperable stage and received only intraoperative biopsies, here no tumor stage or grading could be stated. Survival data were retrieved from the patients' records. Overall survival (OS) was calculated from the date of surgery to the last follow-up or death. Disease-free survival (DFS) was defined from the date of surgery to the date of tumor relapse or last follow-up. All tumors were classified according to the TNM 2020 classification. Gallbladder mucosa from patients who underwent cholecystectomy for cholelithiasis was used as control. Additional tumor samples of PSC-BTC were provided by the Institute of Pathology, University Hospital Essen, Germany for immunohistochemical analysis. Clinical data from this small subset of samples were not available. Therefore, a survival analysis on this cohort was not performed. This study was approved by the ethics committee, University Hospital Bonn (Nr. 417/17, Nr. 27/18, Nr. 233/20). The study was carried out in compliance with the Helsinki declaration.

2.2. TMA construction

A tissue microarray (TMA) was constructed manually. Standard Hematoxylin-Eosin stained 3 μm slides were obtained to identify regions with a high amount of tumor infiltration. For each sample, 4 representative tumor cores of 1 mm diameter were transferred from original FFPE blocks to the TMA blocks. If non-neoplastic tissue was available, also two cores tissue/case were included in the TMA.

2.3. Immunohistochemistry

Immunohistochemistry (IHC) was performed on TMA sections

Table 1
Clinical and pathological data of the patients from UK Bonn included in the study.

Characteristic	Group	No. of patients (%)
Sex (%)	Male	34 (53.1%)
	Female	30 (46.9%)
Age	median	67
	range	38–81
pT (%)	T1	15 (23.4%)
	T2	15 (23.4%)
	T3	28 (43.8%)
	T4	2 (3.1%)
	Tx	4 (6.3%)
pN/cN (%)	N0	34 (53.1%)
	N+	30 (46.9%)
M (%)	M0	50 (78.1%)
	M+	10 (15.6%)
	Mx	4 (6.3%)
G (%)	G1	4 (6.3%)
	G2	35 (54.7%)
	G3	19 (29.7%)
	G4	1 (1.6%)
	Gx	5 (7.8%)
Adjuvant Chemotherapy	No	32 (50%)
	Yes	26 (40.6%)
	Unknown	6 (9.4%)
Tumor localization	iCCA	23 (35.9%)
	pCCA	16 (25%)
	dCCA	15 (23.5%)
	GBC	7 (10.9%)
	Unknown	3 (4.7%)
Histological subtype	Small duct type	36 (55.3%)
	Large duct type	26 (40%)
	mixed	2 (3 %)
Total		64

according to standardized protocols using a monoclonal antibody against SLC7A5 (clone ab20877, Abcam, UK). Briefly, 3 µm sections from TMA blocks were mounted on Tomo® Adhesion Microscope Slides, (Matsunami Glass Ind. LTD, Osaka, Japan). The TMA sections were deparaffinized with xylene (2 × 15 min, VWR International, Fontenay-sous-Bois, France) and rehydrated using decreasing concentrations of graded ethanol (Berkel AHK, Ludwigshafen, Germany) to water (Braun, Melsungen, Germany).

Antigen retrieval was achieved by boiling the slides at 99 °C in citrate buffer at pH 6.0 for 20 min. Immunohistochemistry was performed using the semi-automated platform Autostainer 480 S (Medac, Wedel, Germany). All supplementary reagents were provided by Medac.

2.4. Evaluation of immunoreactivity

SLC7A5/LAT1 positivity was evaluated separately in immune and tumor cells. The staining was considered positive in immune cells if a membranous or cytoplasmic staining was present. Expression in tumor cells was predominantly membranous. Expression in tumor cells was evaluated as the percentage of positive cells. Mean values were calculated for each tumor. For survival analysis, we separated the cases into SLC7A5/LAT1 positive and negative. The percentage of positive immune cells was calculated as the number of stained cells divided by the total number of immune cells. Evaluation of immune reactivity was double-checked by an expert pathologist. The best cut-off value for the survival analysis, segregating BTC cases with good versus poor overall survival, was identified as 2% of positive immune cells. The same criteria was used for analyses using the multivariate Cox proportional-hazard model.

2.5. CODEX acquisition and analysis

A BTC case with high expression of SLC7A5 in tumor cells was assessed for CODEX analysis. Briefly, a formalin-fixed paraffin embedded (FFPE) sample was sectioned into 5 µm thick sections onto a poly-L-lysine-coated coverslips. Heat-mediated antigen retrieval was performed on sections in citrate (pH 6.0) buffer. Sections were then stained using antibodies against SLC7A5/LAT1, CD31, CD4, CD103, pan-CK, Vimentin, CD8, CD68, CD15, CD20, CD15, CD11b, CD14, FAPa, CD11c, CD3e, Foxp3 (Inv), CD45 (details in Suppl. Table 4, using the protocol outlined in Ref. [33]. All antibodies were conjugated in-house to oligonucleotide sequences synthesized by biomers.net GmbH. Stained sections were acquired on a PhenoCycler-Fusion (formerly CODEX; Akoya Biosciences) coupled to a ZEISS Axio Observer 7 inverted microscope through the CODEX Instrument Manager (CIM; Akoya Biosciences) and ZEN (ZEISS) softwares. Sequential cycles each involved the acquisition of DAPI, Atto550, DY-647P1, and DY-747P1.

Images were processed using a combination of existing tools [34–37] and in-house code. Cells were segmented with Cellpose v2 [38] using the cyto2 model fine-tuned with dataset-specific manual annotations. Single-cell fluorescence intensity based features were extracted from the segmented images using in-house code, then high-dimensional embedding and clustering was performed in Scanpy [39] using the Umap and Leiden algorithms respectively. Subsequently, rank markers were calculated for each cluster using Scanpy and algorithmically compared to pre-defined cell type signatures, using a Wilcoxon rank-sum test with cutoff 0 for both test score and log-fold change, and 0.01 for the p-value. Cells belonging to SCL7A5/LAT1 positive immune clusters were analyzed in two representative regions of the tumor (region 1 represents the tumor center and region 2 represents the tumor periphery). Details on cell classification are given in the supplementary tables 1, 2 and 3.

2.6. TCGA analysis

Publicly available TCGA data was accessed through Xena, a cancer genomics data analysis platform [40]. Briefly, the expression of *SLC7A5* was analyzed in TCGA Bile Duct Cancer (CHOL) data set consisting of 45 samples (36 primary tumor and 9 solid tissue normal). Data was downloaded and analyzed with GraphPad Prism (Version 8.0.2; GraphPad Software Inc., Boston, MA, USA).

2.7. Statistical analysis

Statistical analysis was performed with SPSS Statistic version 27 (IBM, Armonk, New York, USA). The primary statistical objective of this study was to evaluate the prognostic value of SCL7A5/LAT1 in sBTC and PSC-BTC by the mean of IHC expression. The Kaplan-Meier method was applied to estimate the event-time distributions for overall survival (OS) and disease-free survival (DFS). Kaplan-Meier curves were compared using the log-rank method. Parameters comparison between groups was made with Mann-Whitney test or ANOVA as appropriate. For correlation analysis, Spearman Rho test and Pearson test were used. For the multivariate analysis we applied the Cox-proportional hazard model.

3. Results

3.1. SLC7A5 is overexpressed in BTC tumors

To assess whether the gene expression of *SLC7A5* is enhanced in BTC tumors, expression was analyzed in TCGA Bile Duct Cancer (CHOL) data set (n = 45; 36 primary tumor and 9 normal adjacent samples). *SLC7A5* gene expression was significantly higher in primary tumor versus adjacent non-neoplastic tissue samples ($p = 0.0002$; Fig. 1A). However, expression did not correlate with overall or progression-free survival. *SLC7A5* encodes an amino acid transporter which could be upregulated by tumor cells to meet the increased biomass demands due to enhanced cellular proliferation. Accordingly, we sought to investigate whether increased expression is associated with upregulation of glucose transporters. Interestingly, the expression of the glucose transporter *SLC2A1* is positively correlated with *SLC7A5* expression (Fig. 1A; Spearman

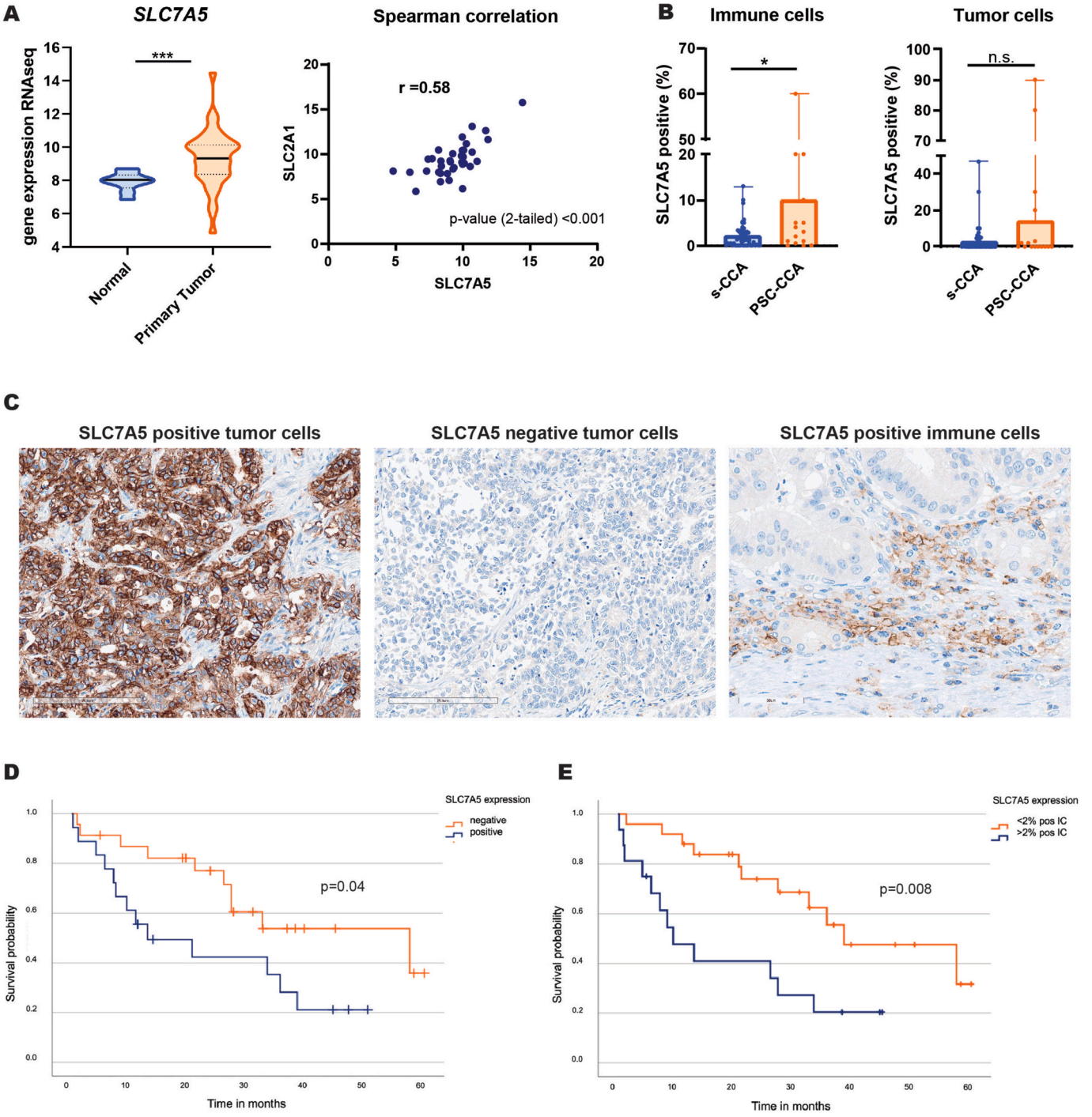

Fig. 1. SLC7A5 in cholangiocarcinoma. A; *SLC7A5* gene expression was analyzed in TCGA Bile Duct Cancer (CHOL) data set (n = 45; 36 primary tumor and 9 normal adjacent samples) via the Xena platform (https://xenabrowser.net/). Left; violin plot depicting the gene expression in tumor versus normal tissue (unpaired *t*-test with Welch's correction p = 0.0002). Right; Spearman correlation between the gene expression of *SLC2A1 and SLC7A5* in primary tumor samples (n = 36). Gene expression RNAseq data is displayed as log2 (norm_count+1). B; scatter bar plots showing the percentage of SLC7A5 positive tumor-infiltrating immune cells (left) and tumor cells (right) in s-BTC versus PSC-BTC. Mann Whitney test p = 0.0411 and p = 0.5783; respectively. C; representative images of SLC7A5 immunoreactivity in BTC. Tumor cell images were taken at a 20× magnification (scale bar represents 200 μm). Immune cell images were taken at a 40× magnification (scale bar represents 60 μm). D; Kaplan Meier plot depicting the overall survival based on SLC7A5 expression in tumor cells in BTC samples (Log Rank-test, p = 0.04). E; Kaplan Meier plot depicting the overall survival time based on the percentage of intratumoral SLC7A5 positive immune cells in BTC (<2 % positive immune cells versus ≥2% positive immune cells; Log Rank-test, p = 0.008).

correlation; r = 0.58).

3.2. Tumoral SLC7A5/LAT1 expression correlates with stage and has prognostic significance in biliary tract cancer

No positivity for SLC7A5/LAT1 was observed in the epithelial cells of non-neoplastic samples. SLC7A5/LAT1 expression was detected mostly

on the cell membrane in tumor cells; on the other hand, membranous and cytoplasmic expression was detected in tumor-infiltrating immune cells with variable intensities (Fig. 1C). Nuclear staining was absent. 30 BTC cases showed SLC7A5/LAT1 positive tumor cells and 39 BTC cases showed SLC7A5/LAT1 negative tumor cells (Table 2). The percentage of SLC7A5/LAT1 positive tumor cells was higher in tumors in advanced stages (T3 and T4) compared with earlier tumor stages (T1 and T2) (Mann-Whitney test, $p = 0.048$). In addition, patients with SLC7A5/LAT1 positive tumors had a significantly shorter OS compared with patients with SLC7A5/LAT1 negative tumors ((LogRank Test, $p = 0.04$) Fig. 1D). The multivariate Cox proportional-hazard model for OS showed no association of SLC7A5/LAT1 positivity on tumor cells and survival (Suppl. Table 5). No statistically significant associations between the percentage of SLC7A5/LAT1 positive tumor cells and tumor localization, tumor grading, lymph node metastasis or distant metastases were noticed. Likewise, Pearson correlation test showed no correlation between the percentage of SLC7A5/LAT1 positive tumor cells and blood parameters, such as neutrophil, lymphocyte, and thrombocyte counts, as well as neutrophil/lymphocyte or lymphocyte/platelet ratios, bilirubin or CRP levels in peripheral blood.

3.3. SLC7A5/LAT1+ tumor-infiltrating immune cells are predominantly found in PSC-BTC

Data regarding SLC7A5/LAT1 expression in PSC-BTC are scarce. To investigate whether SLC7A5/LAT1 could be used as a potential biomarker for PSC-BTC, we compared its expression in PSC-BTC, sBTC, and non-neoplastic tissue in tumor and immune cells. 59 tumor and 9 non-neoplastic samples on TMA and 10 whole slides of PSC-BTC were evaluated for SLC7A5/LAT1 expression. SLC7A5/LAT1 expression was observed in immune cells (4% and 5% respectively) in two non-neoplastic samples. PSC-BTC showed a higher percentage of SLC7A5/LAT1 positive immune cells than sBTC (Mann-Whitney Test, $p = 0.04$, Table 2; Fig. 1B). However, the percentage of SLC7A5/LAT1 -positive tumor cells was not statistically-different between sBTC and PSC-BTC (Fig. 1B).

A significantly higher percentage of SLC7A5/LAT1 + immune cells was noticed in dCCA compared with iCCA (Mann-Whitney test; $p = 0.013$). In addition, a high percentage of SLC7A5/LAT1 positive intratumoral immune cells was associated with a higher concentration of circulating lymphocytes (Spearman Rho; $p = 0.021$) and a low neutrophil/lymphocyte ratio (Spearman Rho; $p = 0.023$). A higher percentage of SLC7A5/LAT1 positive intratumoral immune cells (≥2%) was associated with a significantly shorter overall survival in BTC (Log Rank; $p = 0.008$; Fig. 1E). The multivariate Cox proportional-hazard model for OS did not confirm the higher percentage of SLC7A5 positive intratumoral immune cells as an independent prognostic factor (Suppl. Table 5). No significant association between the percentage of SLC7A5/LAT1 positive tumor-infiltrating immune cells and clinicopathological parameters and disease-free survival time was noticed. Other peripheral blood parameters showed no correlation with the percentage of SLC7A5/LAT1 positive intratumoral immune cells (Pearson correlation test).

Table 2
SLC7A5 positive tumor and immune cells in PSC-BTC and sBTC (UK Bonn and UK Essen).

	PSC-BTC (%)	sBTC (%)	Total
	N	N	N
Tumor cells			
negative	9 (56.2 %)	30 (56.6 %)	39
positive	7 (43.7 %)	23 (43.4 %)	30
Immune cells			
negative	3 (18.7 %)	15 (28.3 %)	18
<2% positive	6 (37.5 %)	31 (58.5 %)	37
≥2% positive	7 (43.7 %)	7 (13.2 %)	14

3.4. Intratumoral infiltration with SLC7A5/LAT1 positive immune cells is a late event in BTC

Since a higher percentage of SLC7A5/LAT1 positive immune cells was observed in PSC-BTC compared to sBTC, we asked whether this is an early event in carcinogenesis or it is related to the late stages.

We analyzed the SLC7A5/LAT1 expression in immune cells adjacent to biliary intraepithelial neoplasia (BilIN) in seven cases included in the study. Here, five cases showed no or less than 2% SLC7A5/LAT1 positive immune cells and two cases had >2% positive immune cells (Suppl. Fig. 1).

3.5. SLC7A5/LAT1 positive immune cells are predominantly CD4$^+$ lymphocytes and macrophages

Next, we asked which immune cell types predominantly express SLC7A5/LAT1 at high levels. To this end, we performed CODEX multiplexed fluorescence microscopy, which allowed us to analyze histological tissue sections by staining multiple fluorescent markers in parallel. Here, we chose a BTC case with high SLC7A5/LAT1 expression in both tumor and immune cells. CODEX fluorescence images showed less immune-cell infiltration in the intratumoral region (Fig. 2A) compared to the peritumoral region (Fig. 2B). CODEX imaging revealed a rich landscape of lymphocyte and myeloid cell populations in both regions (Fig. 2C–E, and Fig. 2F, top), overall accounting for at least 61% of cells (another 19% could not be definitely classified). SLC7A5/LAT1 positive cells were detected in most immune cell compartments, and accounted for 26% of the total immune cell population, which is lower but in a comparable range to the tumor cell compartment (36%). More detailed quantitative analysis revealed that CD4$^+$ T-lymphocytes followed by CD68$^+$ macrophages and CD8$^+$ T-lymphocytes accounted for the largest proportion of SLC7A5/LAT1 positive immune cells (36.6%, 23.1%, and 15.6% of LAT1 positive/Pan-CK negative cells; respectively. Fig. 2F, bottom), while the B-cells detected in the tumor periphery were a minor proportion in the SLC7A5/LAT1 positive population (accounting for 1.2% of LAT1 positive/Pan-CK negative cells). Interestingly, analyzing the percentage of LAT1 expressing cells within each immune cell type showed that CD8$^+$ FOXP3+ regulatory cytotoxic T-lymphocytes (regulatory CTLs) had the highest density (>50%) of SLC7A5/LAT1 positive cells in both analyzed regions (Fig. 2F, middle). Overall, CODEX multiplexed imaging allowed for detailed cartography of SLC7A5/LAT1 positive immune cell compartments in the tumor microenvironment.

4. Discussions

Biliary tract cancers are a heterogeneous group of malignancies characterized by late diagnosis, dismal prognosis, and scarce therapeutic options. Therefore, there is an urgent demand for novel treatment strategies. In the case of PSC-BTC, chronic inflammation with subsequential damage to the epithelium are believed to trigger the progression from low-grade to high-grade dysplasia, and ultimately to invasive carcinoma. However, the exact underlying mechanisms of how inflammation in PSC contributes to PSC-BTC carcinogenesis remain unknown. The lifetime incidence of BTC is reported to be up to 20% in patients with PSC; and PSC-associated BTC patients are significantly younger than patients with sBTC [41–43]. Thus, PSC-BTC patients have a different spectrum of comorbidities that may require distinct therapeutic strategies. The aim of this study was to explore differences in SLC7A5/LAT1 expression between PSC-BTC and sBTC. Analysis of TCGA data showed significantly upregulated SLC7A5/LAT1 expression in primary tumor versus adjacent non-neoplastic tissue samples. Immunohistochemistry analyses showed no statistical differences in the percentage of SLC7A5/LAT1 expressing-tumor cells in PSC-BTC versus sBTC. Nonetheless, the percentage of SLC7A5/LAT1-positive immune cells was significantly higher in PSC-BTC compared to sBTC, which may be a reflection of the inflammatory nature of the predisposing disease in

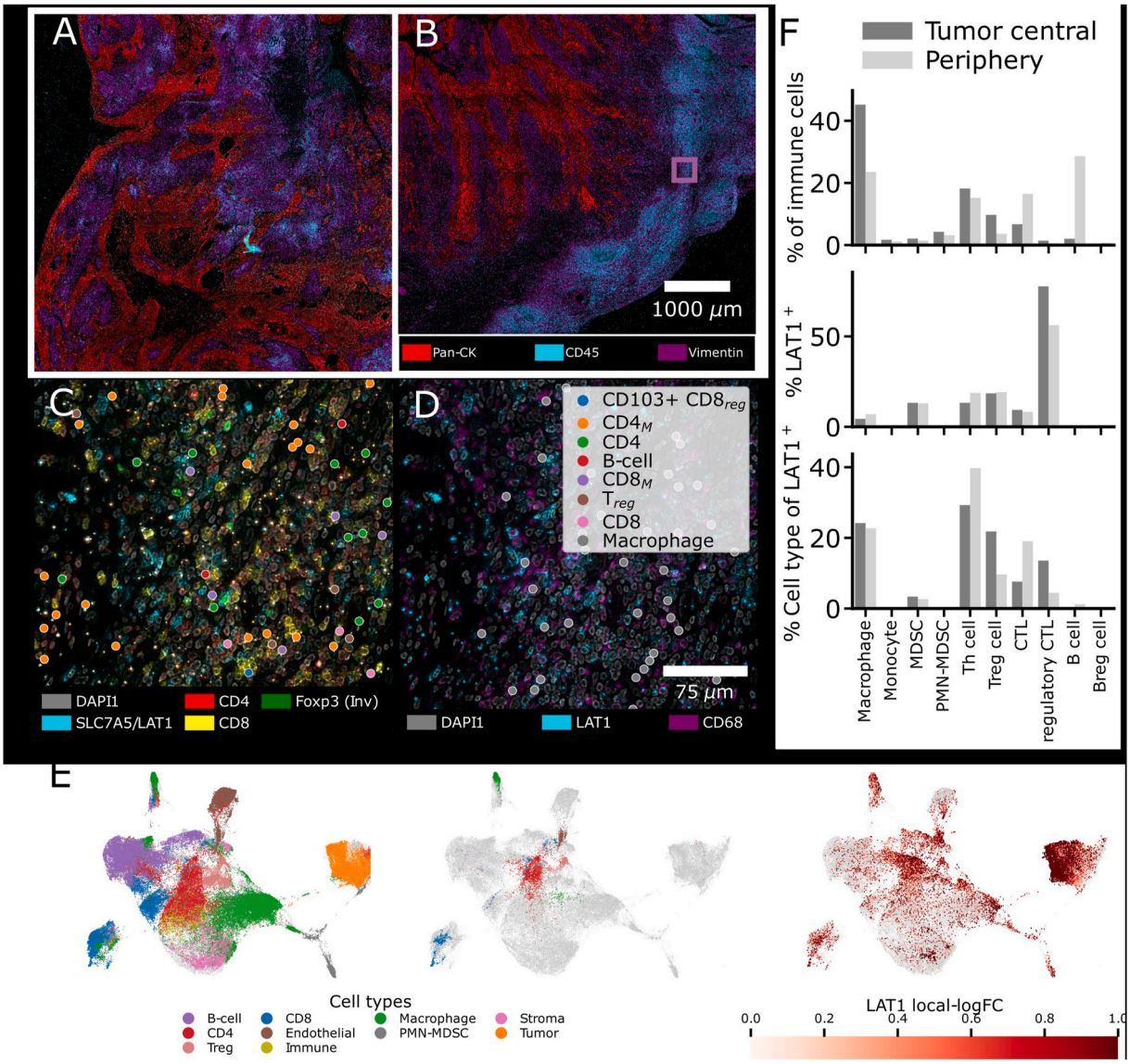

Fig. 2. Codex multiplexed analysis of two representative regions of a cholangiocarcinoma tumor. A; overview of the tumor core sample (slide region 1). B; overview of the tumor periphery sample (slide region 2). C-D; magnified fluorescence images of an immune-cell dense region selected from the tumor periphery (cf. panel B). Shown are (C) the T-cell subpanel with SLC7A5/LAT1 positive lymphocytes indicated by colored makers, and (D) CD68 and SLC7A5/LAT1 signal intensities with SLC7A5/LAT1+ macrophages indicated by colored markers. (E) UMAP embedding showing (left) cell-type annotation, (middle) SLC7A5/LAT1+ immune cells, and (right) the local SLC7A5/LAT1 signal intensity (log fold-change). (F) Distribution of immune cell types in the tumor central and peripheral slide regions, as (top) percentage of all detected cells and (bottom) percentage of all SLC7A5/LAT1+Pan-CK- cells; further (middle), the fraction of SLC7A5/LAT1+ cells within each cell type is shown.

PSC-BTC. Furthermore, SLC7A5/LAT1 expression was positively-correlated with expression of the glucose transporter SLC2A1 in the TCGA dataset. Along these lines, deregulating cellular metabolism is a well-known hallmark of cancer [44]. Due to the rapid proliferation rate and the subsequent increase in nutrient and biomass demands, tumor cells must upregulate one or more amino acid and glucose transporters [45,46]. Similarly, increased amino acid and glucose uptake has been shown to be required by activated T cells for biomass synthesis [47,48]. To this end, the association of SLC7A5/LAT1-positive immune cells with a shorter overall survival could imply that immune cells upregulate the amino acid transporter SLC7A5/LAT1 as a response to a more metabolically-competitive microenvironment.

As revealed by CODEX multiplex immunofluorescence, $CD4^+$ T lymphocytes comprised the largest proportion of SLC7A5/LAT1 positive immune cells, followed by macrophages and $CD8^+$ T-lymphocytes. B-lymphocytes accounted for a minor population of SLC7A5/LAT1 positive immune cells while CD103+ tissue resident T-lymphocytes were totally negative. This is in line with the findings on immune cells revealed by the studies of Yan et al. in breast cancer [28]. SLC7A5/LAT1 positive intratumoral immune cells were associated with a higher concentration of lymphocytes in the peripheral blood, a low neutrophils/lymphocytes ratio, as well as a significantly shorter overall survival. The multivariate Cox proportional-hazard model did not confirm SLC7A5/LAT1 positive intratumoral immune cells as an independent prognostic factor for overall survival. However, this could be due to the relatively small size of our cohort and the challenges that this model can present with when dealing with small sample sizes. The role of SLC7A5/LAT1 in biliary tract cancer was recently highlighted by Kaira et al. and Selenge et al. [25,26], who found that a high expression of SLC7A5/LAT1 on tumor cells was correlated with a shorter disease-free and overall survival. This is in line with our data, showing that patients exhibiting SLC7A5/LAT1 positive tumors had significantly

more advanced stage tumors (T3 and T4) and a shorter overall survival compared with patients with SLC7A5/LAT1 negative tumors. In contrast to the work of Kaira K et al. [25], which found that 64% of biliary tract adenocarcinomas exhibit high SLC7A5/LAT1 expression, in our cohort only 43.5% of cases were positive. This discrepancy could be explained by the different distribution of tumor localization in our cohort.

In conclusion, SLC7A5/LAT1 expression is higher in immune cells infiltrating PSC-BTC compared to sBTC. Moreover, expression of SLC7A5/LAT1 on tumor and immune cells is associated with a shorter overall survival among BTC patients.

Consent and ethics approval

This study was performed with the informed consent of all patients as well as the ethics committee of University Hospital Bonn (No. 417/17, 27/18 and 233/20).

Consent of publication

Not applicable.

Availability of data and materials

The datasets used and/or analyzed during the current study are available from the corresponding author on reasonable request.

Funding

VB received a post-doctoral fellowship grant from the Else-Kröner Fresenius Stiftung (grant number: 2014_Kolleg.05). The study was partially supported by an internal funding provided by Translational Research Area 2 (TRA2) of the University Bonn. MH and KT are supported by Germany's Excellence Strategy (EXC2151-390685813 and EXC2047-390873048). MH, KT and MT are supported by the BMBF-funded e-med program (InterpretTME consortium, Grant Nr. 031L0308A).

CRediT authorship contribution statement

Vittorio Branchi: Writing – review & editing, Writing – original draft, Funding acquisition, Formal analysis, Data curation, Conceptualization. **Racha Hosni:** Writing – review & editing, Writing – original draft, Methodology, Investigation, Formal analysis, Data curation. **Lukas Kiwitz:** Writing – review & editing, Methodology, Investigation, Formal analysis. **Susanna Ng:** Writing – review & editing, Methodology, Investigation, Data curation. **Gemma van der Voort:** Writing – review & editing, Methodology, Investigation, Data curation. **Neila Bambi:** Writing – review & editing, Investigation, Data curation. **Eileen Kleinfelder:** Writing – review & editing, Methodology, Investigation, Formal analysis, Data curation. **Laura K. Esser:** Writing – review & editing, Methodology, Investigation, Data curation. **Leona Dold:** Writing – review & editing, Resources, Conceptualization. **Bettina Langhans:** Writing – review & editing, Resources, Methodology. **Maria A. Gonzalez-Carmona:** Writing – review & editing, Resources, Methodology. **Saskia Ting:** Writing – review & editing, Resources. **Glen Kristiansen:** Writing – review & editing. **Jörg C. Kalff:** Writing – review & editing, Supervision. **Kevin Thurley:** Writing – review & editing, Supervision, Formal analysis. **Michael Hölzel:** Writing – review & editing, Supervision, Formal analysis. **Hanno Matthaei:** Writing – review & editing, Supervision, Data curation. **Marieta I. Toma:** Writing – review & editing, Writing – original draft, Supervision, Conceptualization.

Declaration of competing interest

The authors declare that they have no competing interests.

Acknowledgements

The authors would like to express their gratitude to Seher Aktekin, Kerstin Fuchs, Carsten Golletz and Susanne Steiner for their excellent technical support.

Appendix A. Supplementary data

Supplementary data to this article can be found online at https://doi.org/10.1016/j.humpath.2024.105670.

References

[1] Nakanuma Y, Kakuda Y. Pathologic classification of cholangiocarcinoma: new concepts. Best Pract Res Clin Gastroenterol 2015 Apr 1;29(2):277–93.
[2] Komuta M, Govaere O, Vandecaveye V, Akiba J, Van Steenbergen W, Verslype C, et al. Histological diversity in cholangiocellular carcinoma reflects the different cholangiocyte phenotypes. Hepatology 2012 Jun;55(6):1876–88.
[3] Arai Y, Totoki Y, Hosoda F, Shirota T, Hama N, Nakamura H, et al. Fibroblast growth factor receptor 2 tyrosine kinase fusions define a unique molecular subtype of cholangiocarcinoma. Hepatology 2014 Apr;59(4):1427–34.
[4] Borger DR, Tanabe KK, Fan KC, Lopez HU, Fantin VR, Straley KS, et al. Frequent mutation of isocitrate dehydrogenase (IDH)1 and IDH2 in cholangiocarcinoma identified through broad-based tumor genotyping. Oncol 2012;17(1):72–9.
[5] Graham RP, Barr Fritcher EG, Pestova E, Schulz J, Sitailo LA, Vasmatzis G, et al. Fibroblast growth factor receptor 2 translocations in intrahepatic cholangiocarcinoma. Hum Pathol 2014 Aug 1;45(8):1630–8.
[6] Kipp BR, Voss JS, Kerr SE, Barr Fritcher EG, Graham RP, Zhang L, et al. Isocitrate dehydrogenase 1 and 2 mutations in cholangiocarcinoma. Hum Pathol 2012 Oct;43(10):1552–8.
[7] Lowery MA, Ptashkin R, Jordan E, Berger MF, Zehir A, Capanu M, et al. Comprehensive molecular profiling of intrahepatic and extrahepatic cholangiocarcinomas: potential targets for intervention. Clin Cancer Res 2018 Sep 1;24(17):4154–61.
[8] Nakamura H, Arai Y, Totoki Y, Shirota T, Elzawahry A, Kato M, et al. Genomic spectra of biliary tract cancer. Nat Genet 2015 Sep;47(9):1003–10.
[9] Wang P, Dong Q, Zhang C, Kuan PF, Liu Y, Jeck WR, et al. Mutations in isocitrate dehydrogenase 1 and 2 occur frequently in intrahepatic cholangiocarcinomas and share hypermethylation targets with glioblastomas. Oncogene 2013 Jun 20;32(25):3091–100.
[10] Van Dyke AL, Shiels MS, Jones GS, Pfeiffer RM, Petrick JL, Beebe-Dimmer JL, et al. Biliary tract cancer incidence and trends in the United States by demographic group, 1999-2013. Cancer 2019 May 1;125(9):1489–98.
[11] Rizzo A, Carloni R, Frega G, Palloni A, Di Federico A, Ricci AD, et al. Intensive follow-up program and oncological outcomes of biliary tract cancer patients after curative-intent surgery: a twenty-year experience in a single tertiary medical center. Curr Oncol 2022 Jul 19;29(7):5084–90.
[12] Banales JM, Marin JJG, Lamarca A, Rodrigues PM, Khan SA, Roberts LR, et al. Cholangiocarcinoma 2020: the next horizon in mechanisms and management. Nat Rev Gastroenterol Hepatol 2020 Sep 1;17(9):557–88.
[13] Kim BW, Oh CM, Choi HY, Park JW, Cho H, Ki M. Incidence and overall survival of biliary tract cancers in South Korea from 2006 to 2015: using the national health information database. Gut Liver 2019 Jan 15;13(1):104–13.
[14] Valle J, Wasan H, Palmer DH, Cunningham D, Anthoney A, Maraveyas A, et al. Cisplatin plus gemcitabine versus gemcitabine for biliary tract cancer. N Engl J Med 2010 Apr 8;362(14):1273–81.
[15] Do-Youn Oh, Aiwu Ruth He, Shukui Qin, Li-Tzong Chen, Takuji Okusaka, Vogel Arndt, et al. Durvalumab plus gemcitabine and cisplatin in advanced biliary tract cancer. NEJM Evidence. 2022 Jul 26;1(8):EVIDoa2200015.
[16] Banales JM, Cardinale V, Carpino G, Marzioni M, Andersen JB, Invernizzi P, et al. Expert consensus document: cholangiocarcinoma: current knowledge and future perspectives consensus statement from the European Network for the Study of Cholangiocarcinoma (ENS-CCA). Nat Rev Gastroenterol Hepatol 2016 May;13(5):261–80.
[17] Ceci L, Zhou T, Lenci I, Meadows V, Kennedy L, Li P, et al. Molecular mechanisms linking risk factors to cholangiocarcinoma development. Cancers 2022 Mar 11;14(6):1442.
[18] Tabibian JH, O'Hara SP, Splinter PL, Trussoni CE, LaRusso NF. Cholangiocyte senescence by way of N-ras activation is a characteristic of primary sclerosing cholangitis. Hepatology 2014 Jun;59(6):2263–75.
[19] Kosters A, Karpen SJ. The role of inflammation in cholestasis – clinical and basic aspects. Semin Liver Dis 2010 May;30(2):186–94.
[20] Isomoto H, Kobayashi S, Werneburg NW, Bronk SF, Guicciardi ME, Frank DA, et al. Interleukin 6 upregulates myeloid cell leukemia-1 expression through a STAT3 pathway in cholangiocarcinoma cells. Hepatology 2005;42(6):1329–38.
[21] Goeppert B, Folseraas T, Roessler S, Kloor M, Volckmar AL, Endris V, et al. Genomic characterization of cholangiocarcinoma in primary sclerosing cholangitis reveals therapeutic opportunities. Hepatology 2020 Oct 1;72(4):1253–66.
[22] Kamp EJ, Dinjens WN, Doukas M, van Marion R, Verheij J, Ponsioen CY, et al. Genetic alterations during the neoplastic cascade towards cholangiocarcinoma in primary sclerosing cholangitis. J Pathol 2022 Nov;258(3):227–35.

[23] Scalise M, Galluccio M, Console L, Pochini L, Indiveri C. The human SLC7A5 (LAT1): the intriguing histidine/large neutral amino acid transporter and its relevance to human health. Frontiers in Chemistry [Internet] 2018;6. Available from: https://www.frontiersin.org/article/10.3389/fchem.2018.00243.
[24] Kaira K, Oriuchi N, Imai H, Shimizu K, Yanagitani N, Sunaga N, et al. l-type amino acid transporter 1 and CD98 expression in primary and metastatic sites of human neoplasms. Cancer Sci 2008 Dec;99(12):2380–6.
[25] Kaira K, Sunose Y, Ohshima Y, Ishioka NS, Arakawa K, Ogawa T, et al. Clinical significance of L-type amino acid transporter 1 expression as a prognostic marker and potential of new targeting therapy in biliary tract cancer. BMC Cancer 2013 Oct 16;13:482.
[26] Selenge B, Yamada S, Morine Y, Ikemoto T, Saito Y, Takasu C, et al. Impact of L-type amino acid transporter 1 on intrahepatic cholangiocarcinoma. J Med Invest 2023;70(1.2):160–5.
[27] Nishikubo K, Ohgaki R, Liu X, Okanishi H, Xu M, Endou H, et al. Combination effects of amino acid transporter LAT1 inhibitor nanvuranlat and cytotoxic anticancer drug gemcitabine on pancreatic and biliary tract cancer cells. Cancer Cell Int 2023 Jun 15;23(1):116.
[28] Yan L, He J, Liao X, Liang T, Zhu J, Wei W, et al. A comprehensive analysis of the diagnostic and prognostic value associated with the SLC7A family members in breast cancer. Gland Surg 2022 Feb;11(2):389–411.
[29] Törnroos R, Tina E, Eremo AG. SLC7A5 is linked to increased expression of genes related to proliferation and hypoxia in estrogen-receptor-positive breast cancer. Oncol Rep 2022 Jan;47(1):17.
[30] Tian J, Li X, Jiang Y, Gao F, Ju B, Chen J, et al. SLC7A5 expression is up-regulated in peripheral blood T and B lymphocytes of systemic lupus erythematosus patients, associating with renal damage. Clin Immunol 2022 Apr;237:108987.
[31] Bay C, Bajraktari-Sylejmani G, Haefeli WE, Burhenne J, Weiss J, Sauter M. Functional characterization of the solute carrier LAT-1 (SLC7A5/SLC2A3) in human brain capillary endothelial cells with rapid UPLC-MS/MS quantification of intracellular isotopically labelled L-leucine. Int J Mol Sci 2022 Mar 26;23(7):3637.
[32] Okano N, Naruge D, Kawai K, Kobayashi T, Nagashima F, Endou H, et al. First-in-human phase I study of JPH203, an L-type amino acid transporter 1 inhibitor, in patients with advanced solid tumors. Invest N Drugs 2020 Oct;38(5):1495–506.
[33] Black S, Phillips D, Hickey JW, Kennedy-Darling J, Venkataraaman VG, Samusik N, et al. CODEX multiplexed tissue imaging with DNA-conjugated antibodies. Nat Protoc 2021 Aug;16(8):3802–35.
[34] Czech E, Aksoy BA, Aksoy P, Hammerbacher J. Cytokit: a single-cell analysis toolkit for high dimensional fluorescent microscopy imaging. BMC Bioinf 2019 Sep 2;20(1). https://doi.org/10.1186/s12859-019-3055-3 [Internet]. [cited 2024 Feb 5].
[35] Forster B, Van De Ville D, Berent J, Sage D, Unser M. Complex wavelets for extended depth-of-field: a new method for the fusion of multichannel microscopy images. Microsc Res Tech 2004 Sep;65(1–2):33–42.
[36] Peng T, Thorn K, Schroeder T, Wang L, Theis FJ, Marr C, et al. A BaSiC tool for background and shading correction of optical microscopy images. Nat Commun 2017 Jun 8;8(1). https://doi.org/10.1038/ncomms14836 [Internet]. [cited 2024 Feb 5].
[37] Muhlich JL, Chen YA, Yapp C, Russell D, Santagata S, Sorger PK. Stitching and registering highly multiplexed whole-slide images of tissues and tumors using ASHLAR. Bioinformatics 2022 Aug 16;38(19):4613–21.
[38] Stringer C, Wang T, Michaelos M, Pachitariu M. Cellpose: a generalist algorithm for cellular segmentation. Nat Methods 2020 Dec 14;18(1):100–6.
[39] Wolf FA, Angerer P, Theis FJ. SCANPY: large-scale single-cell gene expression data analysis. Genome Biol 2018 Feb 6;19(1):1–5.
[40] Goldman MJ, Craft B, Hastie M, Repečka K, McDade F, Kamath A, et al. Visualizing and interpreting cancer genomics data via the Xena platform. Nat Biotechnol 2020 Jun;38(6):675–8.
[41] Boonstra K, Weersma RK, van Erpecum KJ, Rauws EA, Spanier BWM, Poen AC, et al. Population-based epidemiology, malignancy risk, and outcome of primary sclerosing cholangitis. Hepatology 2013 Dec;58(6):2045–55.
[42] Weismüller TJ, Trivedi PJ, Bergquist A, Imam M, Lenzen H, Ponsioen CY, et al. Patient age, sex, and inflammatory bowel disease phenotype associate with course of primary sclerosing cholangitis. Gastroenterology 2017 Jun;152(8):1975–1984.e8.
[43] Catanzaro E, Gringeri E, Burra P, Gambato M. Primary sclerosing cholangitis-associated cholangiocarcinoma: from pathogenesis to diagnostic and surveillance strategies. Cancers 2023 Jan;15(20):4947.
[44] Hanahan D. Hallmarks of cancer: new dimensions. Cancer Discov 2022 Jan 12;12(1):31–46.
[45] Bhutia YD, Babu E, Ramachandran S, Ganapathy V. Amino acid transporters in cancer and their relevance to "glutamine addiction": novel targets for the design of a new class of anticancer drugs. Cancer Res 2015 Apr 30;75(9):1782–8.
[46] Ancey PB, Contat C, Meylan E. Glucose transporters in cancer – from tumor cells to the tumor microenvironment. FEBS J 2018;285(16):2926–43.
[47] Hayashi K, Jutabha P, Endou H, Sagara H, Anzai N. LAT1 is a critical transporter of essential amino acids for immune reactions in activated human T cells. J Immunol 2013 Oct 15;191(8):4080–5.
[48] Jacobs SR, Herman CE, Maciver NJ, Wofford JA, Wieman HL, Hammen JJ, et al. Glucose uptake is limiting in T cell activation and requires CD28-mediated Akt-dependent and independent pathways. J Immunol 2008 Apr 1;180(7):4476–86.

4. Discussion with references

As cancer continues to be a disease of high morbidity and mortality, the search for more effective cancer therapeutics and biomarkers remains a critical medical need (Bray et al., 2024). Indeed, there is a tremendous number of newly developed preclinical drug candidates every year; however, few of those candidates successfully pass clinical trials and get implemented into clinical use, which raises questions about the efficacy of the commonly used preclinical models (Kamb, 2005; Sun et al., 2022). This thesis focused on establishing patient-derived organoid models (PDOs) and employing them for investigating potential novel therapeutic targets in cholangiocarcinoma. In addition, patient-derived organoid cultures were established from melanoma brain metastases and were evaluated for predicting targeted-therapy responses based on the mutational profile of the parental tumor. Moreover, the expression of SLC7A5/LAT1, an amino acid transporter that has been shown to correlate to poor prognosis in some cancer entities (Kahlhofer and Teis, 2023), was investigated in cholangiocarcinoma as a potential prognostic biomarker.

4.1 The efficacy of sacituzumab govitecan in cholangiocarcinoma

Novel therapeutic strategies are urgently needed to improve the prognosis of cholangiocarcinoma patients. ADCs have shown enhanced efficacy compared to standard chemotherapeutics in a number of solid tumor entities (Fu et al., 2022; Liu et al., 2024). In my first-author publication (Hosni et al., 2025), we sought to evaluate the expression of the common protein targets of the recently developed ADCs, in cholangiocarcinoma. We assessed the expression of TROP2, NECTIN4, folate receptor 1, HER2, and HER3 in a cholangiocarcinoma cohort (*n*=113). We demonstrated that the TROP2 protein is frequently expressed (91%) in cholangiocarcinoma at moderate to high levels. The other proteins were expressed less commonly (folate receptor 1 (51%), NECTIN4 (49%), HER3 (20%), and HER2 (7%)) and at low levels. Trop2 overexpression has been identified in several solid tumor entities, such as breast, urothelial, lung, gastric, and colorectal cancers (Liu et al., 2022; Loriot et al., 2024). Moreover, we successfully generated PDOs from six cholangiocarcinoma patients and demonstrated their high susceptibility to the cytotoxic

effect of sacituzumab govitecan, *in vitro*. In addition, using two cholangiocarcinoma cell lines, EGI-1 and RBE, we demonstrated induction of apoptosis and cell cycle arrest in response to sacituzumab govitecan and its payload, SN-38, and provided evidence for the dual mechanisms of action of sacituzumab govitecan, the target-dependent and target-independent mechanisms, which highlights the remarkable bystander effect exerted by this ADC. Sacituzumab govitecan (hRS7-CL2A-SN-38; IMMU-132) is a next generation ADC composed of a humanized monoclonal antibody specific to TROP2 (sacituzumab; hRS7) covalently linked to the cytotoxic small-molecule drug payload SN-38 (the active metabolite of irinotecan) via a hydrolyzable linker (CL2A) (Tolaney et al., 2025a). SN-38 works by inhibiting the topoisomerase I enzyme, a central enzyme responsible for maintaining DNA's integrity during DNA replication, and thereby introduces irreversible double-stranded DNA breaks, which leads to cell cycle arrest and apoptosis (Bao et al., 2019; Liu et al., 2000). The SN-38 drug on its own is unsuitable for intravenous infusion, due to its poor solubility and physiological pH-dependent hydrolysis, which led to multiple drug delivery development efforts to overcome these challenges (Chen et al., 2017; Yang et al., 2023). One of the first ADCs that were developed to utilize SN-38's potency and overcome the challenges faced with systemic administration is sacituzumab govitecan (Tolaney et al., 2025a). The SN-38 derivative used in sacituzumab govitecan has improved solubility due to the addition of a polyethylene glycol (PEG) moiety (Goldenberg et al., 2015). Moreover, the linker used binds SN-38 at its active cytotoxic lactone ring which protects it from inactivation. Thus, SN-38 in sacituzumab govitecan is maintained in its active form until released, which enhances its potency and stability (Goldenberg et al., 2015). In line with our data showing the target-dependent and target-independent mechanisms of action, as well as the known systemic release of SN-38, sacituzumab govitecan has been considered as both a prodrug of SN-38 as well as an ADC (Goldenberg et al., 2015; Ocean et al., 2017; Santi et al., 2024, 2021).

This ADC is currently used to treat metastatic triple-negative breast cancer (mTNBC) and HR+/HER2- breast cancer (Tolaney et al., 2025a). Moreover, it is under clinical investigation for the treatment of other cancer entities, such as glioblastoma (NCT04559230), thyroid cancer (NCT06235216), and metastatic colorectal cancer (NCT06243393). Few studies investigating ADCs in cholangiocarcinoma have been published (Kuwatani and Sakamoto, 2023; Yokota et al., 2021; Zhu et al., 2023).

Interestingly, an ongoing non-randomized, open-label, single-arm, phase II clinical trial (NCT06178588), which began in early 2024, is evaluating the anti-tumor activity of sacituzumab govitecan in patients with locally advanced, recurrent, or metastatic cholangiocarcinoma (Kasi et al., 2025). If such initial trials yield positive treatment outcomes, it would be worth evaluating combination therapies with sacituzumab govitecan to assess potential synergistic effects. Combination therapeutic approaches of sacituzumab govitecan with talazoparib, a poly ADP-ribose polymerase (PARP) inhibitor (PARPi), or with pembrolizumab, an immune checkpoint inhibitor targeting PD-1, are under investigation for the treatment of mTNBC (Abelman et al., 2024) (NCT04468061). Due to the single-arm design of the clinical trial assessing the combination of sacituzumab govitecan and talazoparib (Abelman et al., 2024), available data is insufficient to conclude superiority/enhanced efficacy of this combination therapy. NCT04468061 is an ongoing randomized phase II study of sacituzumab govitecan with or without pembrolizumab in PD-L1-negative mTNBC. Interestingly, the ASCENT-04 study, a randomized phase 3 trial testing the combination of sacituzumab govitecan and pembrolizumab versus chemotherapy of physician's choice (gemcitabine + carboplatin, paclitaxel, nab-paclitaxel) and pembrolizumab in PD-L1–positive, advanced unresectable or metastatic TNBC, has reported statistically significant improvement in progression-free survival (PFS) with the combination of sacituzumab govitecan and pembrolizumab (Tolaney et al., 2025b). These results emphasize the enhanced effectiveness of sacituzumab govitecan over standard chemotherapeutics.

Taken together, our data provides preclinical evidence for the potential of using sacituzumab govitecan as a novel therapeutic approach in treating patients with cholangiocarcinoma.

4.2 Modelling targeted therapy responses using PDOs of melanoma brain metastases

In my second publication (Abedellatif et al., 2024), we established a protocol for culturing melanoma brain metastases organoids *in vitro* and demonstrated that the generated organoids preserved the mutational profile of the parental tumor sample. We also showed that the response of the PDOs to treatment with *BRAF* and *MEK* inhibitors matched their mutational profile; cultures with a *BRAF* V600E mutation were sensitive, while cultures with a wildtype *BRAF* were resistant. Given the dismal prognosis of patients with

melanoma brain metastases and the scarcity of representative *in vitro* models available for this disease, this study provides an efficient *in vitro* model for testing targeted therapies, as well as for the discovery of novel therapeutic targets. In line with our data, several studies have used PDOs as an *in vitro* platform to model personalized patient responses; however, no studies using melanoma brain metastases were published at the beginning of our study (Kim et al., 2021; Tan et al., 2023; Wensink et al., 2021). A recently published study demonstrates similar data, albeit using a different culture protocol, and with tumor material from only two 2 patients (Hicks et al., 2024).

4.3 Expression of SLC7A5/LAT1 in BTC

In my third publication (Branchi et al., 2024), the expression of the amino acid transporter SLC7A5/LAT1 was evaluated in sporadic and primary sclerosing cholangitis (PSC)-associated BTC. We found that the gene expression of SLC7A5/LAT1 is upregulated in tumor versus non-neoplastic tissue samples in a cholangiocarcinoma TCGA cohort. Additionally, through analysis of SLC7A5/LAT1 expression via immunohistochemistry in a BTC cohort (69 patients including 16 PSC-associated BTC cases), we observed SLC7A5/LAT1 expression on tumor and intratumoral immune cells in both, sporadic and PSC-associated BTC. Moreover, SLC7A5/LAT1 expression was associated with shorter overall survival and higher tumor stages. This is in line with several published studies showing that SLC7A5/LAT1 is upregulated in several cancer entities and its expression correlates with poor prognosis in some entities (Ichinoe et al., 2011; Kaira et al., 2012, 2008; Sakata et al., 2009). Although the percentage of cases with SLC7A5/LAT1 -positive tumor cells was similar between sporadic and PSC-associated BTC, our analysis showed that the percentage of cases with SLC7A5/LAT1- positive intratumoral immune cells was higher in PSC-associated BTC than in sporadic BTC. The enhanced expression of SLC7A5/LAT1 in intratumoral immune cells in PSC-associated BTC may be a reflection of inflammation and immune activation due to PSC. Indeed, it has been shown that this amino acid transporter is expressed upon activation of human T cells and monocytes/macrophages (Fernández-Gallego et al., 2025; Yoon et al., 2018). Additionally, its central role in the activation of immune cells has been demonstrated by genetic deletion and pharmacologic inhibition in T cells and monocytes/macrophages; respectively, where blocking SLC7A5-mediated amino acid uptake led to a marked reduction in immune

activation (Fernández-Gallego et al., 2025; Yoon et al., 2018). Along these lines, our multiplexed fluorescence microscopy analysis of a BTC sample with high SLC7A5/LAT1 expression, in both tumor and immune cells, revealed that CD4+ T-lymphocytes, followed by CD68+ macrophages and CD8+ T-lymphocytes, accounted for the largest proportion of SLC7A5/LAT1 positive immune cells. Taken together, the data from this study proposes that SLC7A5/LAT1 could represent a prognostic biomarker in BTC, and demonstrates differences in the immune cells' phenotype between sporadic and PSC-associated BTC.

4.4 References

Abedellatif, S.-E., Hosni, R., Waha, A., Gielen, G.H., Banat, M., Hamed, M., Güresir, E., Fröhlich, A., Sirokay, J., Wulf, A.-L., Kristiansen, G., Pietsch, T., Vatter, H., Hölzel, M., Schneider, M., Toma, M.I., 2024. Melanoma Brain Metastases Patient-Derived Organoids: An In Vitro Platform for Drug Screening. Pharmaceutics 16, 1042. https://doi.org/10.3390/pharmaceutics16081042

Abelman, R.O., Spring, L., Niemierko, A., Abraham, E., McNeice, M., Goff, J., Valenti, A., Wander, S.A., Isakoff, S.J., Moy, B., Juric, D., Vidula, N., Waks, A.G., Parsons, H.A., Ellisen, L.W., Tolaney, S.M., Bardia, A., 2024. Sequential combination of sacituzumab govitecan and talazoparib in metastatic triple negative breast cancer (mTNBC): Results from a phase II study. JCO 42, 1102–1102. https://doi.org/10.1200/JCO.2024.42.16_suppl.1102

Bao, X., Wu, J., Kim, S., LoRusso, P., Li, J., 2019. Pharmacometabolomics Reveals Irinotecan Mechanism of Action in Cancer Patients. J Clin Pharmacol 59, 20–34. https://doi.org/10.1002/jcph.1275

Branchi, V., Hosni, R., Kiwitz, L., Ng, S., van der Voort, G., Bambi, N., Kleinfelder, E., Esser, L.K., Dold, L., Langhans, B., Gonzalez-Carmona, M.A., Ting, S., Kristiansen, G., Kalff, J.C., Thurley, K., Hölzel, M., Matthaei, H., Toma, M.I., 2024. Expression of the large amino acid transporter SLC7A5/LAT1 on immune cells is enhanced in primary sclerosing cholangitis-associated cholangiocarcinoma and correlates with poor prognosis in cholangiocarcinoma. Human Pathology 153, 105670. https://doi.org/10.1016/j.humpath.2024.105670

Bray, F., Laversanne, M., Sung, H., Ferlay, J., Siegel, R.L., Soerjomataram, I., Jemal, A., 2024. Global cancer statistics 2022: GLOBOCAN estimates of incidence and mortality worldwide for 36 cancers in 185 countries. CA: A Cancer Journal for Clinicians 74, 229–263. https://doi.org/10.3322/caac.21834

Chen, M., Li, W., Zhang, X., Dong, Y., Hua, Y., Zhang, H., Gao, J., Zhao, L., Li, Y., Zheng, A., 2017. In vitro and in vivo evaluation of SN-38 nanocrystals with different particle sizes. International Journal of Nanomedicine 12, 5487–5500. https://doi.org/10.2147/IJN.S133816

Fernández-Gallego, N., Anega, B., Luengo-Arias, S., Bizkarguenaga, M., Gil-Redondo, R., Embade, N., Navarrete-Arias, L., Ramírez-Huesca, M., Álvarez-Corrales, E., Dosil, S.G., Castillo-González, R., Rojas-Gomez, A., Espeleta, I., Martínez-Martínez, S., Alfranca, A., G de Yebenes, V., Martín-Cófreces, N.B., Aragonés, J., Martin, P., Millet, O., Sánchez-Madrid, F., Cibrian, D., 2025. Restricting SLC7A5-mediated Leucine uptake in T cells prevents acute GVHD and maintains GVT response. EMBO Molecular Medicine 17, 1631–1665. https://doi.org/10.1038/s44321-025-00250-2

Fu, Z., Li, S., Han, S., Shi, C., Zhang, Y., 2022. Antibody drug conjugate: the “biological missile” for targeted cancer therapy. Sig Transduct Target Ther 7, 1–25. https://doi.org/10.1038/s41392-022-00947-7

Goldenberg, D.M., Cardillo, T.M., Govindan, S.V., Rossi, E.A., Sharkey, R.M., 2015. Trop-2 is a novel target for solid cancer therapy with sacituzumab govitecan (IMMU-132), an antibody-drug conjugate (ADC). Oncotarget 6, 22496–22512. https://doi.org/10.18632/oncotarget.4318

Hicks, W.H., Gattie, L.C., Shami, M.E., Traylor, J.I., Davar, D., Najjar, Y.G., Richardson, T.E., McBrayer, S.K., Abdullah, K.G., 2024. Matched three-dimensional organoids and two-dimensional cell lines of melanoma brain metastases mirror response to targeted molecular therapy. Sci Rep 14, 24843. https://doi.org/10.1038/s41598-024-76583-8

Hosni, R., Klümper, N., Sanders, C., Hosni, S., Branchi, V., Semaan, A., Alajati, A., Pelusi, N., Ng, S.S., Ralser, D.J., Abedellatif, S.-E., Matthaei, H., Kalff, J., Boovadira Poonacha, J., Lukacs-Kornek, V., Kristiansen, G., Gonzalez-Carmona, M.A., Hölzel, M., Toma, M.I., 2025. The Antibody–Drug Conjugate Sacituzumab Govitecan (IMMU-132) Represents a Potential Novel Therapeutic Strategy in Cholangiocarcinoma. Molecular Cancer Therapeutics OF1–OF14. https://doi.org/10.1158/1535-7163.MCT-24-0972

Ichinoe, M., Mikami, T., Yoshida, T., Igawa, I., Tsuruta, T., Nakada, N., Anzai, N., Suzuki, Y., Endou, H., Okayasu, I., 2011. High expression of L-type amino-acid transporter 1 (LAT1) in gastric carcinomas: comparison with non-cancerous lesions. Pathol Int 61, 281–289. https://doi.org/10.1111/j.1440-1827.2011.02650.x

Kahlhofer, J., Teis, D., 2023. The human LAT1–4F2hc (SLC7A5–SLC3A2) transporter complex: Physiological and pathophysiological implications. Basic & Clinical Pharmacology & Toxicology 133, 459–472. https://doi.org/10.1111/bcpt.13821

Kaira, K., Oriuchi, N., Imai, H., Shimizu, K., Yanagitani, N., Sunaga, N., Hisada, T., Tanaka, S., Ishizuka, T., Kanai, Y., Endou, H., Nakajima, T., Mori, M., 2008. Prognostic significance of L-type amino acid transporter 1 expression in resectable stage I-III nonsmall cell lung cancer. Br J Cancer 98, 742–748. https://doi.org/10.1038/sj.bjc.6604235

Kaira, K., Sunose, Y., Arakawa, K., Ogawa, T., Sunaga, N., Shimizu, K., Tominaga, H., Oriuchi, N., Itoh, H., Nagamori, S., Kanai, Y., Segawa, A., Furuya, M., Mori, M., Oyama, T., Takeyoshi, I., 2012. Prognostic significance of L-type amino-acid transporter 1 expression in surgically resected pancreatic cancer. Br J Cancer 107, 632–638. https://doi.org/10.1038/bjc.2012.310

Kamb, A., 2005. What’s wrong with our cancer models? Nat Rev Drug Discov 4, 161–165. https://doi.org/10.1038/nrd1635

Kasi, A., Al-Rajabi, R.M.T., Li, H., Carroll, E., Bradbury, S., Broxterman, C., Phadnis, M.A., Baranda, J.C., Sun, W., 2025. A phase II open-label study of sacituzumab

govitecan in patients with previously treated locally advanced, recurrent, or metastatic cholangiocarcinoma (SIGNA). JCO 43, TPS651–TPS651. https://doi.org/10.1200/JCO.2025.43.4_suppl.TPS651

Kim, S.-Y., Kim, S.-M., Lim, S., Lee, J.Y., Choi, S.-J., Yang, S.-D., Yun, M.R., Kim, C.G., Gu, S.R., Park, C., Park, A.-Y., Lim, S.M., Heo, S.G., Kim, H., Cho, B.C., 2021. Modeling Clinical Responses to Targeted Therapies by Patient-Derived Organoids of Advanced Lung Adenocarcinoma. Clin Cancer Res 27, 4397–4409. https://doi.org/10.1158/1078-0432.CCR-20-5026

Kuwatani, M., Sakamoto, N., 2023. Promising Highly Targeted Therapies for Cholangiocarcinoma: A Review and Future Perspectives. Cancers (Basel) 15, 3686. https://doi.org/10.3390/cancers15143686

Liu, K., Li, M., Li, Yudong, Li, Yutong, Chen, Z., Tang, Y., Yang, M., Deng, G., Liu, H., 2024. A review of the clinical efficacy of FDA-approved antibody–drug conjugates in human cancers. Molecular Cancer 23, 62. https://doi.org/10.1186/s12943-024-01963-7

Liu, L.F., Desai, S.D., Li, T.-K., Mao, Y., Sun, M., Sim, S.-P., 2000. Mechanism of Action of Camptothecin. Annals of the New York Academy of Sciences 922, 1–10. https://doi.org/10.1111/j.1749-6632.2000.tb07020.x

Liu, X., Deng, J., Yuan, Y., Chen, W., Sun, W., Wang, Y., Huang, H., Liang, B., Ming, T., Wen, J., Huang, B., Xing, D., 2022. Advances in Trop2-targeted therapy: Novel agents and opportunities beyond breast cancer. Pharmacology & Therapeutics 239, 108296. https://doi.org/10.1016/j.pharmthera.2022.108296

Loriot, Y., Balar, A.V., Petrylak, D.P., Kalebasty, A.R., Grivas, P., Fléchon, A., Jain, R.K., Swami, U., Bupathi, M., Barthélémy, P., Beuzeboc, P., Palmbos, P., Kyriakopoulos, C.E., Pouessel, D., Sternberg, C.N., Tonelli, J., Sierecki, M., Zavodovskaya, M., Elboudwarej, E., Diehl, L., Jürgensmeier, J.M., Tagawa, S.T., 2024. Sacituzumab Govitecan Demonstrates Efficacy across Tumor Trop-2 Expression Levels in Patients with Advanced Urothelial Cancer. Clin Cancer Res 30, 3179–3188. https://doi.org/10.1158/1078-0432.CCR-23-3924

Ocean, A.J., Starodub, A.N., Bardia, A., Vahdat, L.T., Isakoff, S.J., Guarino, M., Messersmith, W.A., Picozzi, V.J., Mayer, I.A., Wegener, W.A., Maliakal, P., Govindan, S.V., Sharkey, R.M., Goldenberg, D.M., 2017. Sacituzumab govitecan (IMMU-132), an anti-Trop-2-SN-38 antibody-drug conjugate for the treatment of diverse epithelial cancers: Safety and pharmacokinetics. Cancer 123, 3843–3854. https://doi.org/10.1002/cncr.30789

Sakata, T., Ferdous, G., Tsuruta, T., Satoh, T., Baba, S., Muto, T., Ueno, A., Kanai, Y., Endou, H., Okayasu, I., 2009. L-type amino-acid transporter 1 as a novel biomarker for high-grade malignancy in prostate cancer. Pathol Int 59, 7–18. https://doi.org/10.1111/j.1440-1827.2008.02319.x

Santi, D.V., Ashley, G.W., Cabel, L., Bidard, F.-C., 2024. Could a Long-Acting Prodrug of SN-38 be Efficacious in Sacituzumab Govitecan-Resistant Tumors? BioDrugs 38, 171–176. https://doi.org/10.1007/s40259-024-00643-8

Santi, D.V., Cabel, L., Bidard, F.-C., 2021. Does sacituzumab-govitecan act as a conventional antibody drug conjugate (ADC), a prodrug of SN-38 or both? Ann Transl Med 9, 1113. https://doi.org/10.21037/atm-21-1103

Sun, D., Gao, W., Hu, H., Zhou, S., 2022. Why 90% of clinical drug development fails and how to improve it? Acta Pharm Sin B 12, 3049–3062. https://doi.org/10.1016/j.apsb.2022.02.002

Tan, T., Mouradov, D., Lee, M., Gard, G., Hirokawa, Y., Li, S., Lin, C., Li, F., Luo, H., Wu, K., Palmieri, M., Leong, E., Clarke, J., Sakthianandeswaren, A., Brasier, H., Tie, J., Tebbutt, N.C., Jalali, A., Wong, R., Burgess, A.W., Gibbs, P., Sieber, O.M., 2023. Unified framework for patient-derived, tumor-organoid-based predictive testing of standard-of-care therapies in metastatic colorectal cancer. CR Med 4. https://doi.org/10.1016/j.xcrm.2023.101335

Tolaney, S.M., Cardillo, T.M., Chou, C.-C., Dornan, C., Faris, M., 2025a. The Mode of Action and Clinical Outcomes of Sacituzumab Govitecan in Solid Tumors. Clin Cancer Res 31, 1390–1399. https://doi.org/10.1158/1078-0432.CCR-24-1525

Tolaney, S.M., de Azambuja, E., Kalinsky, K., Loi, S., Kim, S.-B., Yam, C., Rapoport, B.L., Im, S.-A., Pistilli, B., McHayleh, W., Cescon, D.W., Watanabe, J., Lara, A., Freitas-Junior, R., Bofill, J.S., Afshari, M., Gary, D., Wang, L., Lai, C., Schmid, P., 2025b. Sacituzumab govitecan (SG) + pembrolizumab (pembro) vs chemotherapy (chemo) + pembro in previously untreated PD-L1–positive advanced triple-negative breast cancer (TNBC): Primary results from the randomized phase 3 ASCENT-04/KEYNOTE-D19 study. JCO 43, LBA109–LBA109. https://doi.org/10.1200/JCO.2025.43.17_suppl.LBA109

Wensink, G.E., Elias, S.G., Mullenders, J., Koopman, M., Boj, S.F., Kranenburg, O.W., Roodhart, J.M.L., 2021. Patient-derived organoids as a predictive biomarker for treatment response in cancer patients. npj Precis. Onc. 5, 30. https://doi.org/10.1038/s41698-021-00168-1

Yang, J., Jia, L., He, Z., Wang, Y., 2023. Recent advances in SN-38 drug delivery system. International Journal of Pharmaceutics 637, 122886. https://doi.org/10.1016/j.ijpharm.2023.122886

Yokota, K., Serada, S., Tsujii, S., Toya, K., Takahashi, T., Matsunaga, T., Fujimoto, M., Uemura, S., Namikawa, T., Murakami, I., Kobayashi, S., Eguchi, H., Doki, Y., Hanazaki, K., Naka, T., 2021. Anti-Glypican-1 Antibody–drug Conjugate as Potential Therapy Against Tumor Cells and Tumor Vasculature for Glypican-1–Positive Cholangiocarcinoma. Molecular Cancer Therapeutics 20, 1713–1722. https://doi.org/10.1158/1535-7163.MCT-21-0015

Yoon, B.R., Oh, Y.-J., Kang, S.W., Lee, E.B., Lee, W.-W., 2018. Role of SLC7A5 in Metabolic Reprogramming of Human Monocyte/Macrophage Immune Responses. Front Immunol 9, 53. https://doi.org/10.3389/fimmu.2018.00053

Zhu, B., Wang, X., Shimura, T., Huang, A.C., Kong, N., Dai, Y., Fang, J., Guo, P., Ying, J.-E., 2023. Development of potent antibody drug conjugates against ICAM1+ cancer cells in preclinical models of cholangiocarcinoma. npj Precis. Onc. 7, 1–13. https://doi.org/10.1038/s41698-023-00447-z

5. Acknowledgments

I would like to deeply thank my primary supervisor, Prof. Dr. med Marieta Toma, for giving me the opportunity for conducting my PhD work in her lab, and for guiding me throughout the way. I would like to thank Prof. Dr. med Michael Hölzel and Dr. Niklas Klümper for giving me critical feedback. I would like to thank my other doctoral committee members, Prof. Dr. Eva Kiermaier and Prof. Dr. Hubert Schorle, for their interest in reviewing my doctoral work. I would like to extend my acknowledgments to Prof. Dr. Glen Kristiansen, the director of the Institute of Pathology, for welcoming me in his institute and for his critical feedback during the institute seminars. I would also like to thank the medical and technical staff of the institute for their precious help in obtaining and processing human tissue samples. I would like to thank the patients, included in my studies, for consenting to the use of parts of their samples for the sake of research. Last but not least, I would like to thank my family members for their tremendous support.

6. Statement on own contribution

The work was carried out at the Institute of Pathology under the supervision of Prof. Dr. med Marieta Toma.

The first publication “The Antibody–Drug Conjugate Sacituzumab Govitecan (IMMU-132) Represents a Potential Novel Therapeutic Strategy in Cholangiocarcinoma” was conceptualized by Prof. Dr. med Marieta Toma and Dr. Niklas Klümper. I was responsible for designing, planning, performing, and analyzing the experimental work. Additionally, I prepared the graphs and figures, and wrote the manuscript. Analysis and evaluation of histopathology slides were done with the support of my supervisor, Prof. Dr. med Marieta Toma. Anonymized patient data collection was done by Dr. Vittorio Branchi and Dr. Alexander Semaan. I interpreted the data with the support of my supervisors, Prof. Dr. med Marieta Toma and Prof. Dr. med Michael Hölzel.

The second publication “Melanoma Brain Metastases Patient-Derived Organoids: An In Vitro Platform for Drug Screening” was conceptualized by Prof. Dr. med Marieta Toma and Saif-Eldin Abedellatif (Dr. med candidate at the time of the study and the first author of the publication). I contributed by supporting the first author, Saif-Eldin Abedellatif, in planning and designing experiments, data analysis and interpretation, and critical revision and editing of the manuscript.

The third publication “Expression of the large amino acid transporter SLC7A5/LAT1 on immune cells is enhanced in primary sclerosing cholangitis-associated cholangiocarcinoma and correlates with poor prognosis in cholangiocarcinoma” was conceptualized by Prof. Dr. med Marieta Toma, Dr. Vittorio Branchi, and Prof. Dr. med Michael Hölzel. I performed TCGA cohort (publicly-available) data analysis, prepared figure 1 parts A, B, and C, and wrote some parts of the manuscript. Dr. Vittorio Branchi collected patient’s data. Lukas Kiwitz, Dr. Susanna Ng and Gemma van der Voort performed immunofluorescence staining and analysis. Prof. Dr. Marieta Toma and Dr. Vittorio Branchi evaluated patients’ data with respect to clinic-pathological characteristics.

I confirm that I have written this thesis independently and have not used any sources or aids other than those specified by me.